



Estimating real-time traffic state of holding vehicles at signalized intersections using partial connected vehicle trajectory data

Shaocheng Jia ^a, S.C. Wong ^{a,*}, Wai Wong ^{b,**}

^a Department of Civil Engineering, The University of Hong Kong, Hong Kong, PR China

^b Department of Civil and Natural Resources Engineering, University of Canterbury, Christchurch 8041, New Zealand



ARTICLE INFO

Keywords:

Connected vehicle
Penetration rate
Traffic state estimation
Holding vehicle estimation
Signalized intersection

ABSTRACT

Emerging connected vehicle (CV) technologies offer unprecedented opportunities to estimate various traffic states, enhancing traffic management and control. Among these states, a particularly critical yet underexplored one is the number of holding vehicles—vehicles that, based on their projected trajectories using cruise speed, should have been discharged at any instant of interest but are instead impeded and remain undischarged. Accurately estimating this quantity is essential for real-time traffic state monitoring and control, as it directly reflects the effectiveness of traffic flow at intersections. However, the prolonged transition period implies a mix of CVs and non-connected vehicles (NCs) within transportation networks, resulting in incomplete traffic information. To address this challenge, this paper proposes a generic and fully analytical CV-based holding vehicle (CVHV) model to estimate the number of holding vehicles at any instant of interest, relying solely on partial CV trajectory data. The CVHV model accommodates any signal plans, CV penetration rates, and traffic demands. Two sub-models, CVHV-I and CVHV-II, are derived to account for different holding vehicle patterns at any instant of interest falling within the effective red or green of a signal group, respectively. Each sub-model handles various holding vehicle patterns, including holding vehicle components such as stopped holding CVs and NCs, and moving holding CVs and NCs. Comprehensive numerical experiments in VISSIM validate the effectiveness of the CVHV model under varying volume-to-capacity ratios, CV penetration rates, and signal timing configurations. Its practical applicability is further demonstrated using the real-world Next Generation Simulation dataset. Additionally, the application of the proposed model to estimating the real-time total number of vehicles in a lane and to a simple illustrative example of CV-based adaptive signal control highlights the significance of accurately estimating the traffic state of holding vehicles.

1. Introduction

The emergence of fifth-generation (5G) mobile communication, known for its ultra-low latency (0.01 s) and reliable information exchange (Tahir and Katz 2022), has facilitated the development of advanced connected vehicle (CV) technologies, including vehicle-to-vehicle (V2V) and vehicle-to-infrastructure (V2I) systems. CVs can transmit their travel information through basic safety messages, which include timestamps, locations, speeds, accelerations, and heading directions. The availability of these CV data presents

* Corresponding author at: Department of Civil Engineering, The University of Hong Kong, Hong Kong, PR China.

** Corresponding author at: Department of Civil and Natural Resources Engineering, University of Canterbury, Christchurch 8041, New Zealand.

E-mail addresses: hhecwsc@hku.hk (S.C. Wong), wai.wong@canterbury.ac.nz (W. Wong).

unprecedented opportunities to enhance the efficiency, mobility, and resilience of transportation networks through various beneficial applications. However, the transition to full CV deployment is expected to be a prolonged process that may experience challenges related to privacy, willingness-to-share, and policies that prevent its complete realization. Consequently, there will be an extended period of transition during which both CVs and non-connected vehicles (NCs) coexist within the transportation network. This implies that complete traffic information will not be readily available and will need to be inferred from the partial data provided by CVs, taking into account the CV penetration rates.

The CV penetration rate is defined as the proportion of CV flow to total traffic flow and is essential for inferring complete traffic information. In cases where fixed detectors are installed on roads, obtaining the total traffic flow is relatively straightforward, and by combining the CV flow with the total flow, the CV penetration rate can be easily estimated. However, detectors are not present on all of the links on a road network and they can be non-functional when undergoing occasional maintenance or due to other technical problems. This problem can be solved by devising a simple but useful model that uses a certain distribution to represent CV penetration rates across different links within a road network (Wong and Wong, 2015, 2016a, 2019; Wong et al., 2019a). This means that sample CV penetration rates from links equipped with detectors can be used to estimate the mean and variance of the distribution. Subsequently, based on the principle of geographical proximity, the estimated mean is used as an estimate of the CV penetration rate on links without detectors. Nevertheless, the hidden assumption of independent and identically distributed CV penetration rates across different links can be violated due to differences between land uses and correlations between links. Attempts have been made to account for CV penetration rate variability based on different land-use properties (Meng et al., 2017), but the use of local data in the development of the relevant model limits its generalizability.

The single-source data approach has gained significant attention in recent years, due to its being more flexible and practical than the multi-source data approach. For example, under the assumption of Poisson arrivals, Comert (2016) derived several analytical models for estimating CV penetration rate using CV data. However, such an assumption may not always hold in reality. Wong et al. (2019b) overcame this shortcoming by deriving the first unbiased estimator for CV penetration rate based solely on CV data. This analytical and non-parametric method does not make any assumptions about arrival patterns. Zhao et al. (2019a, 2019b, 2022) have used maximum likelihood estimation (MLE) to estimate vehicle stopping position distributions and CV penetration rates. However, all of the aforementioned methods are point estimators and thus could introduce bias into transport models and suboptimal solutions in optimizations, given the dynamic and nonlinear nature of transportation systems (Wong and Wong, 2015, 2016a, 2019; Wong et al., 2019a; Yin, 2008). Jia et al. (2023) circumvented these limitations by extending the work of Wong et al. (2019) to devise an exact probabilistic penetration rate (PPR) model, which accurately quantifies the uncertainty in CV penetration rates. This model provides a systematic analysis framework for CV-based applications and lays a solid foundation for CV-based stochastic modeling and optimization.

The availability of CV penetration rates has enabled numerous transportation applications, such as estimation of queue length (Comert and Cetin 2009, 2011; Comert 2013; Hao et al., 2014); estimation of arrival table (Feng et al., 2015; Jenelius and Koutopoulos, 2013, 2015; Rahmani et al., 2015; Tian et al., 2015; Khan et al., 2017; Mousa et al., 2017; Iqbal et al., 2018; Lu et al., 2019); estimation of traffic flow (Wong and Wong, 2015, 2016a, 2016c); estimation of traffic density (Geroliminis and Daganzo, 2008; Ambühl and Menendez, 2016; Du et al., 2016; Wong and Wong, 2019; Wong et al., 2019a, 2021); estimation of origin–destination patterns (Yang et al., 2017; Wang et al., 2020; Cao et al., 2021); adaptive signal control (Feng et al., 2015; Jia et al., 2025); and evaluation of traffic incident impacts (Wong and Wong, 2016b).

Recently, the CV penetration rate (Wong et al., 2019b) and its variability (Jia et al., 2023) have been incorporated into stochastic models to support a wide range of CV-based applications. Among these, adaptive traffic signal control has received increasing attention due to its potential to optimize signal operations based on real-time traffic states inferred from CV data. In the context of adaptive

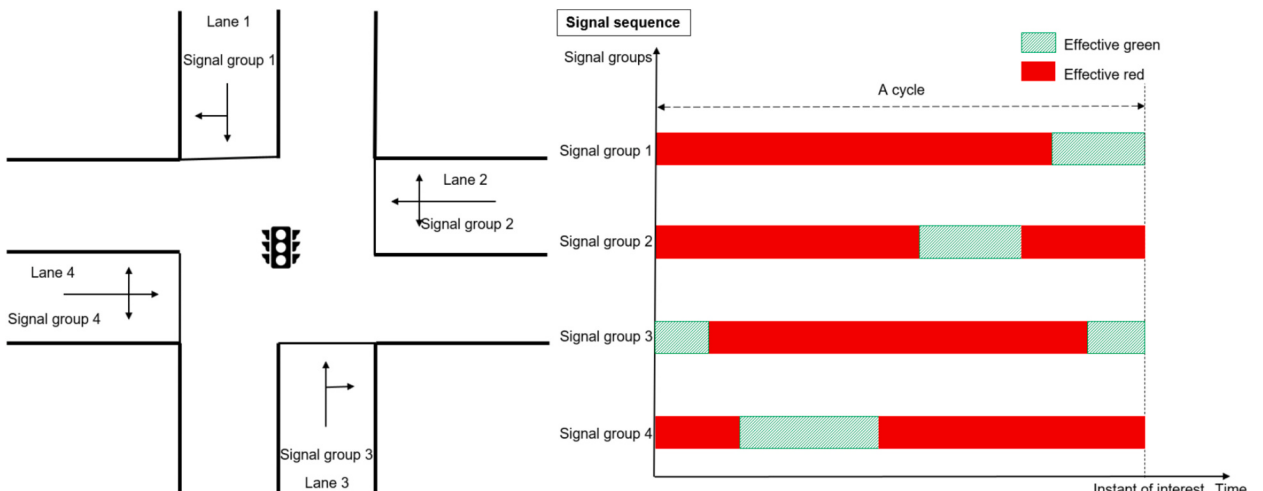


Fig. 1. Illustration of an instant of interest falling within the effective red and green of different signal groups.

traffic signal control, regardless of the specific control logic employed, the fundamental objective is to optimize signal plans in real time to handle all vehicles approaching an intersection. To achieve this, a critical requirement is the real-time estimation of the total number of vehicles across all approaches at any given instant of interest. This total can be broadly decomposed into two categories: (1) undischarged vehicles, which should have already departed the system based on their projected trajectories using their cruise speeds but have not yet done so; and (2) newly arriving vehicles, which are not projected to be discharged at that instant. Undischarged vehicles have been partially addressed in classical traffic flow theory through the notion of residual queue. Specifically, residual queue refers to vehicles that, based on their projected trajectories using cruise speed, should have been discharged at the end of the green phase, but are instead held by the system and remain undischarged. However, this concept is limited to a specific temporal boundary: the end of a green phase. As a result, it does not support estimation of undischarged vehicles at any arbitrary points in time. For instance, consider a signalized intersection controlled by multiple signal groups, as illustrated in Fig. 1. A signal cycle is defined from the start of the effective red to the end of the effective green of signal group 1. If an instant of interest falls at the end of this cycle, it lies within the effective green of signal groups 1 and 3 and the effective red of signal groups 2 and 4. In such a scenario, the classical residual queue definition fails to capture undischarged vehicles for signal groups 2, 3, and 4, thereby limiting the capability and feasibility of real-time traffic state monitoring for adaptive control.

To address this gap, a generalization of the residual queue concept is proposed by extending it beyond fixed temporal boundaries to any moment in time. To avoid confusion with the existing term, the notion of holding vehicles is introduced. A holding vehicle is defined as any vehicle that, based on its projected trajectory using its cruise speed, should have been discharged at any instant of interest but is instead held by the system and remain undischarged (Jia et al., 2025). This broader definition allows for more comprehensive monitoring of system states across all signal groups at any instant. Notably, the classical residual queue can be viewed as a special case of holding vehicles, applicable only at the end of a green phase. By contrast, the holding vehicle can also be viewed as a generalization of the residual queue concept. As such, it provides a robust, flexible and unifying framework for monitoring and estimating real-time traffic states at signalized intersections.

The practical significance of holding vehicles is evident in applications of adaptive signal control. For instance, Jia et al. (2024a, 2024b) modeled the number of holding vehicles at the end of effective green as a Markov process, developing a residual-vehicle (RV) model to derive the stationary distribution as the long-term holding vehicle distribution. This approach, applied to a simple stochastic CV-based adaptive signal control scheme, demonstrated that incorporating holding vehicles improves delay estimation and signal performance. Compared to a scheme ignoring holding vehicles, the RV-informed scheme reduced average delays by up to 7.8 % and 42.3 %, maximum delays by up to 12.7 % and 71.2 %, and delay variations by up to 34.6 % and 89.2 % for intersections with volume-to-capacity (V/C) ratios of 0.61 and 0.92, respectively, at a CV penetration rate of 0.4. These findings underscore the critical role of holding vehicle estimation in optimizing traffic efficiency. However, the RV model is limited to the special case of residual vehicles at the end of effective green and provides only long-term distributions, not real-time estimates at any arbitrary instant of interest.

Modeling holding vehicles at any instant of interest poses significant challenges due to their complex dynamics. Unlike new arrivals, which typically move in a free-flow state with minimal interactions, holding vehicles may be stopped, decelerating, or recovering from a prior stop, influenced by signal timing and vehicle interactions. This complexity complicates the development of a generic, real-time estimation model. Yet, it also presents opportunities: the rich interactions among holding vehicles could be leveraged by dedicated models to enhance accuracy, improving real-time estimation of total vehicle numbers and supporting intelligent transportation system (ITS) applications such as vehicle location and speed estimation (Feng et al., 2015) and max-pressure control (Varaiya, 2013).

However, conventional traffic systems relying on fixed detectors face significant limitations in estimating the number of holding vehicles. Loop detectors, for instance, can only capture traffic states (such as speed, location, and acceleration) at specific points on the roadway and cannot account for conditions upstream or downstream. This lack of spatial coverage makes it particularly difficult to detect undischarged vehicles. Additionally, estimating the numbers of holding vehicles on links without detectors poses an even greater challenge. By contrast, emerging CV technologies offer high-resolution, spatiotemporal data that can track vehicle trajectories across the entire network. This capability presents a promising avenue for real-time estimation of holding vehicles. However, despite this potential, no existing methods have been developed to leverage CV data for estimating the number of holding vehicles at any arbitrary time instant of interest. This highlights a critical research gap: the need for a real-time, generic method for estimating the number of holding vehicles at any instant of interest that fully utilizes the capabilities of CV data.

This study aims to bridge the aforementioned research gap by developing a holding vehicle estimation method that relies exclusively on partially available CV trajectory data. To estimate the number of holding vehicles, crucial inputs include the CV penetration rate and arrival rate, which are simultaneously estimated using maximum likelihood estimation (MLE). Subsequently, the CV-based holding vehicle (CVHV) model, which consists of two sub-models—the CVHV-I sub-model and the CVHV-II sub-model—is developed. The CVHV-I sub-model captures the holding vehicle patterns at an instant of interest falling within the effective red of a signal group, while the CVHV-II sub-model captures the holding vehicle patterns at an instant of interest falling within the effective green of a signal group. Each sub-model comprises a set of analytical models that effectively capture various holding vehicle components, such as numbers of stopped holding CVs and NCs, and moving holding CVs and NCs. These models were tested through extensive VISSIM simulations and further validated in a real-world scenario based on the Next Generation Simulation (NGSIM) dataset (Federal Highway Administration, 2006). The application of the proposed CVHV model to estimate the real-time total number of vehicles in a lane, along with a simple illustrative example of CV-based adaptive signal control, demonstrates the significance of accurately modeling holding vehicles for real-time ITS applications.

The remaining sections of this paper are structured as follows. Section 2 presents the problem statement and introduces the notation used throughout this paper. Section 3 details the CVHV model. Section 4 presents the results of numerical experiments conducted on

the VISSIM platform. [Section 5](#) describes the validation of the models performed using the NGSIM dataset. [Section 6](#) presents two example applications where the number of holding vehicles in a lane is used as an essential input, highlighting the importance of accurately estimating holding vehicles. Finally, [Section 7](#) concludes the paper by summarizing the findings and highlighting the contributions of this research.

2. Problem statement and notation

2.1. Problem statement

Consider approaches connecting to an intersection with multiple traffic streams controlled by different signal groups in a signal plan. The instant of interest can fall within either the effective red (e.g., signal groups 2 and 4 in [Fig. 1](#)) or effective green (e.g., signal groups 1 and 3 in [Fig. 1](#)) of a signal group. Without loss of generality, signal groups can be categorized into cases based on whether the

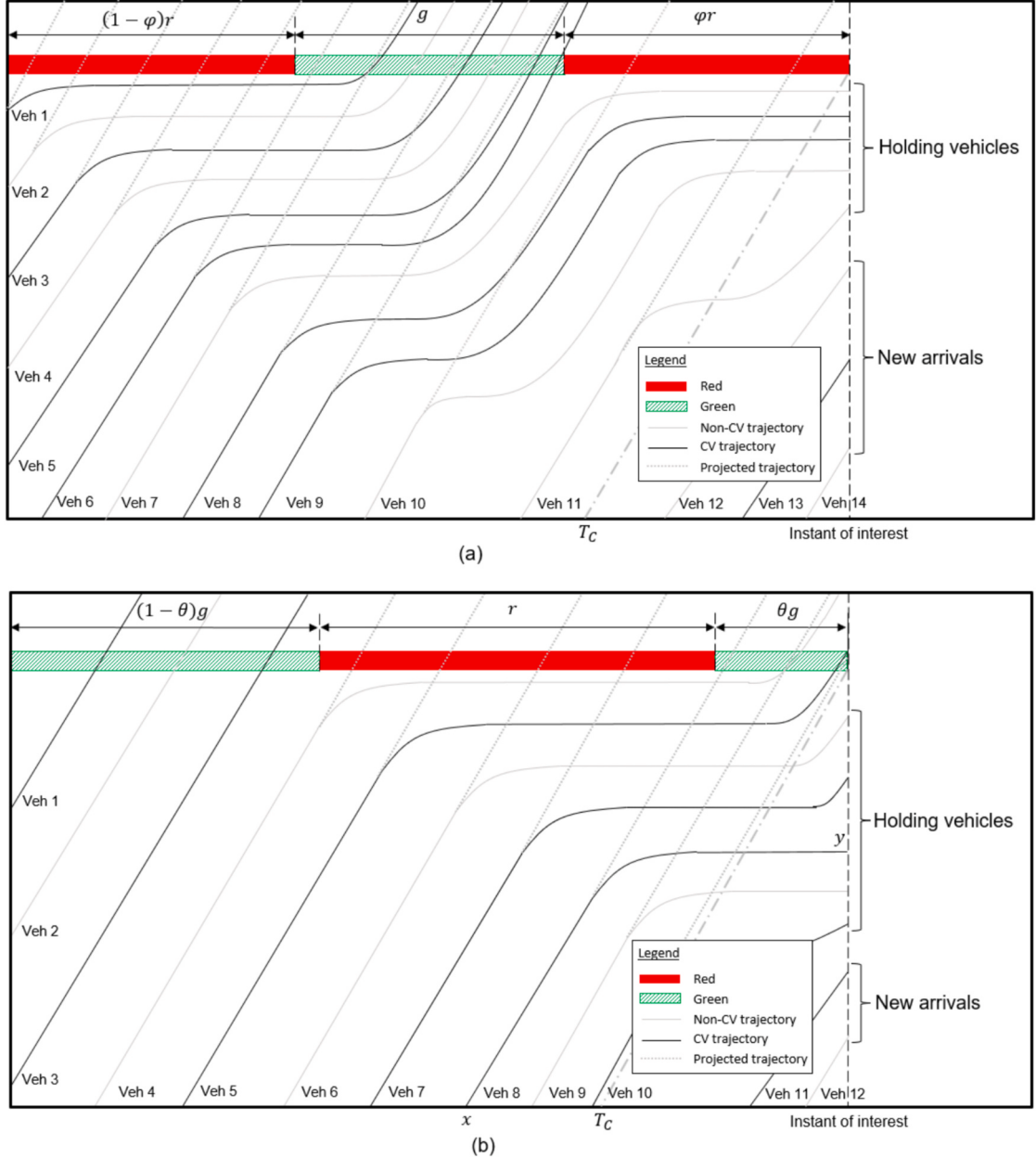


Fig. 2. Holding vehicle patterns: (a) instant of interest falls within the effective red of a signal group, and (b) instant of interest falls within the effective green of a signal group.

instant of interest falls within their effective red or green, and these cases are generically represented by the settings illustrated in Fig. 2(a) and 2(b), respectively. Parameters φ and θ , ranging from 0 to 1, locate the instant of interest falling within the effective red and effective green of a signal group, respectively. Cases with $\varphi = 1$ and $\theta = 1$ represent the special cases of instants of interest at the end of effective red and green, respectively.

In this flexible framework, holding vehicles in a lane at any instant of interest are generically defined as vehicles that, based on their projected trajectories using cruise speed, should have been discharged at that instant but are instead held by the system and remain undischarged. It is important to emphasize that this definition extends beyond the classical notion of residual queue in traffic flow theory, which applies specifically to undischarged vehicles remaining at the end of an effective green phase. Notably, when $\varphi = 0$ or $\theta = 1$, holding vehicles are equivalent to residual queue. In this way, the residual queue can be regarded as a special case of holding vehicles. Conversely, the holding vehicle concept serves as a natural generalization of the residual queue, enabling broader and continuous monitoring of undischarged vehicles across time. In Fig. 2(a), vehicles 7, 8, 9, 10, and 11 were projected to discharge before the instant of interest; however, they remained undischarged at the instant of interest, forming the holding vehicle set {7, 8, 9, 10, 11}. Similarly, in Fig. 2(b), vehicles 6, 7, 8, 9, and 10 were anticipated to discharge before the instant of interest based on their projected trajectories, but they persisted at the instant of interest as holding vehicles. It is evident that the patterns of holding vehicles differ depending on whether the instant of interest falls within the effective red or green of a signal group. In the former case, the number of holding vehicles is typically expected to be non-zero due to the red period φr with a holding vehicle set of {7, 8, 9, 10, 11} in Fig. 2(a). This holding vehicle set comprises the stopped holding vehicle set, {7, 8, 9, 10}, and the moving holding vehicle set, {11}. Stopped holding vehicles are those with a speed of zero at the instant of interest. In the latter case, holding vehicles may still exist if there is incomplete discharge due to a short green period θg or temporarily high demand. As shown in Fig. 2(b), the holding vehicle set, {6, 7, 8, 9, 10}, is a union of a moving holding vehicle set, {6, 7}, a stopped holding vehicle set, {8, 9}, and another moving holding vehicle set, {10}. Thus, these holding vehicle sets can consist of a combination of stopped CVs and non-CVs, and moving CVs and non-CVs. Furthermore, in a connected environment, only partial CV information is available. In addition, there are diverse combinations of holding vehicle components and signal timings. The aforementioned factors increase the complexity of estimating the numbers of holding vehicles in all controlling lanes at an instant of interest under this flexible framework. Hence, the objective of this paper is to develop a method that accurately estimates the number of holding vehicles, considering any given signal timings, and relying solely on time, speed, and location data reported by CVs.

2.2. Notations

Table 1 lists the notation for parameters or variables used in this paper.

In addition, the following sets are defined:

Table 1

Notation.

Notation	Description	Example (Fig. 2(b))
R	The number of holding vehicles at an instant of interest	$R = 5$
R_1	The sum of the number of holding vehicles located before the last stopped holding CV plus this CV in a holding vehicle set	$R_1 = 3$
R_2	The number of remaining holding vehicles that are not included in R_1 , i.e., $R - R_1$	$R_2 = 2$
$V^{(1)}$	The set of stopped holding CVs at an instant of interest	$V^{(1)} = \{8\}$
$V^{(2)}$	The set of moving holding CVs at an instant of interest	$V^{(2)} = \{7, 10\}$
$V_j^{(i)}$	The j^{th} CV in $V^{(i)}$	$V_1^{(1)} = 8$
$V^{(2,1)}$	The set of holding CVs in $V^{(2)}$ located before the stopped holding CVs	$V^{(2,1)} = \{7\}$
$V^{(2,2)}$	The set of holding CVs in $V^{(2)}$ located after the stopped holding CVs	$V^{(2,2)} = \{10\}$
$T^{(i)}$	The set of instants at which CVs in $V^{(i)}$ enter the link	$T^{(1)} = \{x\}$
$T_j^{(i)}$	The instant at which $V_j^{(i)}$ enters the link	$T_1^{(1)} = x$
$L^{(i)}$	The set of locations where CVs in $V^{(i)}$ are located at an instant of interest	$L^{(1)} = \{y\}$
$L_j^{(i)}$	The location of $V_j^{(i)}$, measured from the upstream intersection to the front bumper of $V_j^{(i)}$, at an instant of interest	$L_1^{(1)} = y$
l	Link length	—
l_e	Average effective vehicle length	—
T_C	Projected instant of interest at upstream	—
s	Saturation flow rate	—
g	Effective green	—
θ	Signal segmentation parameter locating the instant of interest within the effective green	—
r	Effective red	—
φ	Signal segmentation parameter locating the instant of interest within the effective red	—
C	Cycle length	—
T^*	Cruise time (expected travel time from upstream to downstream)	—
\bar{q}	Average arrival rate	—
\bar{q}_N	Average arrival rate for NCs	—
\bar{p}	Average CV penetration rate	—
v_f	Cruise speed	—

$$V^{(i)} = \left\{ V_1^{(i)}, V_2^{(i)}, V_3^{(i)}, \dots, V_j^{(i)}, \dots, V_{k_i}^{(i)} \right\}, \forall i = 1, 2 \text{ and } \forall j \in [1, k_i], \quad (1)$$

$$T^{(i)} = \left\{ T_1^{(i)}, T_2^{(i)}, T_3^{(i)}, \dots, T_j^{(i)}, \dots, T_{k_i}^{(i)} \right\}, \forall i = 1, 2 \text{ and } \forall j \in [1, k_i], \quad (2)$$

$$L^{(i)} = \left\{ L_1^{(i)}, L_2^{(i)}, L_3^{(i)}, \dots, L_j^{(i)}, \dots, L_{k_i}^{(i)} \right\}, \forall i = 1, 2 \text{ and } \forall j \in [1, k_i], \quad (3)$$

$$V^{(2,1)} = \left\{ V_1^{(2)}, V_2^{(2)}, V_3^{(2)}, \dots, V_u^{(2)}, \dots, V_m^{(2)} \right\}, \forall u \in [1, m] \quad (4)$$

$$V^{(2,2)} = \left\{ V_{m+1}^{(2)}, V_{m+2}^{(2)}, V_{m+3}^{(2)}, \dots, V_v^{(2)}, \dots, V_{k_2}^{(2)} \right\}, \forall v \in [m+1, k_2]. \quad (5)$$

In Eq. (1), when $i = 1$, $V^{(1)}$ represents the set of stopped holding CVs at an instant of interest, and $V_j^{(1)}$ is the j^{th} CV in $V^{(1)}$, $\forall j \in [1, k_1]$. When $i = 2$, $V^{(2)}$ represents the set of moving holding CVs at an instant of interest, and $V_j^{(2)}$ is the j^{th} CV in $V^{(2)}$, $\forall j \in [1, k_2]$. In Eq. (2), $T^{(i)}$ is the set of instants when CVs in $V^{(i)}$ enter the link, $\forall i \in [1, 2]$, and $T_j^{(i)}$ is the j^{th} instant in $T^{(i)}$, $\forall j \in [1, k_i]$. Similarly, in Eq. (3), $L^{(i)}$ is the set of locations where CVs in $V^{(i)}$ are located at an instant of interest, $\forall i \in [1, 2]$, and $L_j^{(i)}$ is the j^{th} location in $L^{(i)}$, $\forall j \in [1, k_i]$. Eq. (4) and Eq. (5) divide $V^{(2)}$ into $V^{(2,1)}$ and $V^{(2,2)}$, which represent the moving holding CV sets before and after the stopped holding CVs, respectively. $V_u^{(2)}$ is the u^{th} CV in $V^{(2,1)}$, $\forall u \in [1, m]$, and $V_v^{(2)}$ is the v^{th} CV in $V^{(2,2)}$, $\forall v \in [m+1, k_2]$.

3. Methodology

This section introduces the CVHV model for estimating the number of holding vehicles. The average CV penetration rate and arrival rate, which are essential inputs for the CVHV model, are first estimated. Two sub-models of the CVHV model—the CVHV-I sub-model and the CVHV-II sub-model—are then introduced. The CVHV-I sub-model estimates the holding vehicle patterns at an instant of interest that falls within the effective red of a signal group, whereas the CVHV-II sub-model estimates the holding vehicle patterns at an instant of interest that falls within their effective green of a signal group. The foundational assumption underlying the derivation of the proposed models asserts that CVs and NCs are sufficiently well-mixed. This mixing process is represented by the frequent lane-changing and overtaking maneuvers (Wong et al. 2019). Under this assumption, each vehicle is assigned probabilities \bar{p} and $1 - \bar{p}$ to be a CV and an NC, respectively.

3.1. Estimation of \bar{p} and \bar{q}

Consider a lane connected to a signalized intersection, where some vehicles are required to stop (i.e., to have a speed of zero) at an instant due to red signals, forming a constrained queue. A constrained queue is a spatiotemporal concept defined as a set of vehicles stopped by a red signal. Further details on constrained queues can be found in Wong et al. (2019b) and Jia et al. (2023, 2024a, 2024b). The numbers of CVs and vehicles stopped before the last CV in a constrained queue are denoted as n and \tilde{N} , respectively, and can be easily estimated using the average effective vehicle length, l_e (Wong et al., 2019b; Jia et al., 2023, 2024a, 2024b). However, as the vehicles after the last CV are unobservable, \tilde{N} represents only a partial constrained queue length. Given that the full constrained queue length, N , follows a certain distribution (i.e., $P(N = i) = \pi_i, \forall i = 0, 1, 2, \dots, k$) and that n follows a binomial distribution (i.e., $n \sim B(N, \bar{p})$), the joint probability distribution of n and \tilde{N} is given as follows (Jia et al., 2023):

$$P(n = i, \tilde{N} = j) = \begin{cases} \pi_0 + \sum_{z=1}^k \pi_z (1 - \bar{p})^z, & i = 0, j = 0 \\ \sum_{z=j}^k \pi_z \binom{j-1}{i-1} \bar{p}^i (1 - \bar{p})^{z-i}, & \forall i, j = 1, 2, \dots, k, j \geq i \end{cases}, \quad (6)$$

The distribution of N can be estimated using either the Probabilistic Dissipation Time (PDT) model or the Constant Dissipation Time (CDT) model (Jia et al. 2023). The PDT model, as demonstrated below, has the ability to accurately estimate the constrained queue length distribution, albeit with a comparatively higher level of complexity.

$$P(N = k) = \begin{cases} f(k; \bar{q}t) f(0; \bar{q}kt) + \\ \sum_{i=1}^{k-1} \sum_{j=1}^{J_i} f(i; \bar{q}t) \tilde{P}_j(N = k, M = i) W_j(N = k, M = i), \text{ if } k \in \mathbb{N}^+, \\ f(0; \bar{q}t), \text{ if } k = 0 \end{cases}, \quad (7)$$

where $f(k; \bar{q}t)$ represents the probability of k arriving vehicles with the average arrival rate \bar{q} during t and is determined by the vehicle arrival pattern; $\tilde{P}_j(N = k, M = i)$ and $W_j(N = k, M = i)$, $\forall j \in [1, J_i]$ can be obtained through Algorithm 1 as shown in Appendix A. Conversely, the CDT model simplifies the PDT model by assuming that N follows a Poisson distribution with parameter λ ,

which quantitatively equals the average constrained queue length N_0 and can be estimated by $\lambda = N_0 = s\bar{q}r/(s - \bar{q})$.

The above analysis implies that n and \tilde{N} are dependent on both \bar{q} and \bar{p} .

\bar{p} . Let n_i and \tilde{N}_i denote the numbers of CVs and observable vehicles, respectively, in the constrained queue formed in cycle i . Then, based on Eq. (6), the following MLE formulation can be established:

$$\max_{\bar{q}, \bar{p}} \prod_{j=0}^{\Psi} P(n_{i-j}, \tilde{N}_{i-j}), \quad (8)$$

where $\Psi = 0, 1, 2, \dots, i-1$ and represents the number of past cycles considered in the likelihood function. As there are two control variables, \bar{q}, \bar{p} , only, a simple grid search method is employed to solve Eq. (8) and search for the optimal solution. This method exhibits high computational efficiency when dealing with analytical likelihood functions. The optimal solution provides the most probable estimates for the average arrival rate and CV penetration rate, denoted as \bar{q}^* and \bar{p}^* , respectively. For the sake of brevity, \bar{q} and \bar{p} are used to represent the optimal solution from the MLE in the subsequent sections.

3.2. CVHV-I sub-model

This subsection focuses on the derivation of the CVHV-I sub-model, which models the holding vehicle patterns at an instant of interest falling within the effective red of a signal group. A set of analytical models **Propositions 1–4** is devised that take into account various possible holding vehicle patterns and thereby ensure that accurate estimates of the number of holding vehicles are obtained.

Proposition 1. Given that $V^{(1)} \neq \emptyset$ and $V^{(2)} = \emptyset$ in a lane at an instant falling within the effective red of a signal group, the number of holding vehicles in this lane at this instant, R , can be estimated as follows:

$$R = \frac{l - L_{k_1}^{(1)}}{l_e} + \bar{q}(1 - \bar{p})(T_C - T_{k_1}^{(1)}) + 1. \quad (9)$$

Proof. The fact that $V^{(1)} \neq \emptyset$ implies that there is at least one stopped holding CV present behind the stop bar. Thus, the number of holding vehicles located before the last stopped holding CV, including it, R_1 , can be estimated as follows:

$$R_1 = \frac{l - L_{k_1}^{(1)}}{l_e} + 1, \quad (10)$$

where l , $L_{k_1}^{(1)}$, and l_e represent the link length, the location of $V_{k_1}^{(1)}$ measured from the upstream intersection to the front bumper of $V_{k_1}^{(1)}$, and the average effective vehicle length, respectively. The first term in Eq. (10) estimates the number of vehicles between the stop bar and $V_{k_1}^{(1)}$, excluding $V_{k_1}^{(1)}$.

The fact that $V^{(2)} = \emptyset$ means that there is no moving CV after the stopped holding CVs. However, there may still be stopped or moving holding NCs after the last stopped holding CV. For example, in Fig. 2(a), vehicles 10 and 11 are holding NCs and can be counted as follows.

$$R_2 = \bar{q}_N(T_C - T_{k_1}^{(1)}), \quad (11)$$

where \bar{q}_N represents the average arrival rate of NCs and is estimated by

$$\bar{q}_N = \bar{q}(1 - \bar{p}); \quad (12)$$

and $T_C - T_{k_1}^{(1)}$ is the time interval for vehicle arrival estimation. Eq. (11) estimates the expected arrivals during a period based on the product of the average arrival rate and the length of the time interval.

Thus, the number of holding vehicles, R , is given by

$$R = R_1 + R_2 = \frac{l - L_{k_1}^{(1)}}{l_e} + \bar{q}_N(T_C - T_{k_1}^{(1)}) + 1. \quad (13)$$

Substituting Eq. (12) into Eq. (13) affords Eq. (9). Q.E.D.

Proposition 2. Given that $V^{(1)} \neq \emptyset$ and $V^{(2)} \neq \emptyset$ in a lane at an instant falling within the effective red of a signal group, the number of holding vehicles in this lane at this instant, R , can be estimated as follows:

$$R = \frac{l - L_{k_1}^{(1)}}{l_e} + \min \left\{ \bar{q}(1 - \bar{p})(T_1^{(2)} - T_{k_1}^{(1)}), \frac{L_{k_1}^{(1)} - L_1^{(2)}}{l_e} - 1 \right\} + B_2^{k_2} + E + k_2 + 1, \quad (14)$$

where $B_i^j = \sum_{i'}^j \min \left\{ \bar{q}_N(T_j^{(2)} - T_{i'-1}^{(2)}), \frac{L_{j-1}^{(2)} - L_j^{(2)}}{l_e} - 1 \right\}$, and $E = \bar{q}(1 - \bar{p})(T_C - T_{k_2}^{(2)})$. For the sake of brevity, B_i^j and E are used in the subsequent content without further explanation.

Proof. As $V^{(1)} \neq \emptyset$, the proof for the number of holding vehicles located before the last stopped holding CV, including it, R_1 , is identical to that in **Proposition 1**.

However, the number of remaining holding vehicles that are not included in R_1 , i.e., R_2 , must also be estimated. This involves multiple components. First, the number of holding vehicles between $V_{k_1}^{(1)}$ and $V_1^{(2)}$, including $V_1^{(2)}$, are denoted as $R_{2,1}$. In addition, the vehicles in between $V_{k_1}^{(1)}$ and $V_1^{(2)}$, if any, must be NCs. Thus, $R_{2,1}$ can be estimated as follows:

$$R_{2,1} = \bar{q}_N \left(T_1^{(2)} - T_{k_1}^{(1)} \right) + 1, \quad (15)$$

where $T_1^{(2)}$ and $T_{k_1}^{(1)}$ represent the entrance times of $V_1^{(2)}$ and $V_{k_1}^{(1)}$, respectively. Furthermore, the physical size constraint implies that **Axiom 1** must hold.

Axiom 1 Given the distance between two vehicles in a lane, d , and the average effective vehicle length, l_e , the number of vehicles between these two vehicles, excluding them, denoted as χ , must satisfy the following inequality:

$$\chi \leq \frac{d}{l_e} - 1. \quad (16)$$

Proof. The proof of **Axiom 1** is self-evident.

Thus, $R_{2,1}$ is modified as follows:

$$R_{2,1} = \min \left\{ \bar{q}_N \left(T_1^{(2)} - T_{k_1}^{(1)} \right), \frac{L_{k_1}^{(1)} - L_1^{(2)}}{l_e} - 1 \right\} + 1. \quad (17)$$

Similarly, the number of holding vehicles between $V_{j-1}^{(2)}$ and $V_j^{(2)}$, including $V_j^{(2)}$, denoted as $R_{2,j}$, $\forall j = 2, 3, \dots, k_2$, can be estimated as follows:

$$R_{2,j} = \min \left\{ \bar{q}_N \left(T_j^{(2)} - T_{j-1}^{(2)} \right), \frac{L_{j-1}^{(2)} - L_j^{(2)}}{l_e} - 1 \right\} + 1. \quad (18)$$

The number of holding vehicles after $V_{k_2}^{(2)}$, denoted as R_{2,k_2+1} , can be estimated as follows:

$$R_{2,k_2+1} = \bar{q}_N \left(T_C - T_{k_2}^{(2)} \right). \quad (19)$$

Thus, by combining all of these components, R_2 is derived as follows:

$$R_2 = \sum_{j=1}^{k_2+1} R_{2,j}. \quad (20)$$

Therefore, the number of holding vehicles, R , is given by

$$R = R_1 + R_2 = \frac{l - L_{k_1}^{(1)}}{l_e} + 1 + \sum_{j=1}^{k_2+1} R_{2,j}. \quad (21)$$

Substituting Eqs. (12), (17), (18), and (19) into Eq. (21) affords Eq. (14). Q.E.D.

Proposition 3. As $V^{(1)} = \emptyset$ and $V^{(2)} \neq \emptyset$ in a lane at an instant falling within the effective red of a signal group, the number of holding vehicles in this lane at this instant, R , can be estimated as follows:

$$R = \min \left\{ \max \left\{ R_{2,1,k} + \bar{q}_N \left[T_1^{(2)} - (T_C - \varphi r) \right], 0 \right\}, \frac{l - L_1^{(2)}}{l_e} \right\} + B_2^{k_2} + E + k_2, \quad (22)$$

where $k = \lceil (T_C + T^* - t_0)/C \rceil$, $\bar{q}_N = \bar{q}(1 - \bar{p})$, and

$$R_{2,1,j+1} = \begin{cases} \max \{ [T_C - (k-1)C - \varphi r - t_0] \bar{q}_N - s[T_C + T^* - (k-1)C - \varphi r - t_0], 0 \}, & j = 0 \\ \max \{ R_{2,1,j} + \bar{q}_N C - sg, 0 \}, & j > 0 \end{cases}. \quad (23)$$

Proof. The fact that $V^{(1)} = \emptyset$ implies that there is no stopped holding CV and thus $R_1 = 0$.

Multiple components need to be considered to determine R_2 . The first component is the number of holding vehicles prior to the first moving holding CV, denoted as $R_{2,1}$. Let T_0 and t_0 represent the entry and exit times, respectively, of the last CV (e.g., vehicle 6 in Fig. 2 (a)) discharged into a link. Depending on the value of t_0 , it may be necessary to trace back multiple cycles from the current time to estimate $R_{2,1}$. For instance, if $t_0 \in [T_C + T^* - \varphi r - g, T_C + T^* - \varphi r]$, the estimation of $R_{2,1}$ involves only the traffic in $t \in [T_C + T^* - C, T_C + T^*]$. However, if $t_0 < T_C + T^* - \varphi r - g$, the estimation of $R_{2,1}$ involves traffic before $t = T_C + T^* - C$. Let $k = \lceil (T_C + T^* - t_0)/C \rceil$ represent the number of cycles involved in estimating $R_{2,1}$, where $\lceil \bullet \rceil$ represents a ceiling function. Therefore, the

number of holding vehicles at $t = T_C + T^* - (k-1)C - \varphi r$, denoted as $R_{2,1,1}$, is estimated as follows:

$$R_{2,1,1} = \max\{[T_C - (k-1)C - \varphi r - T_0] \bar{q}_N - s[T_C + T^* - (k-1)C - \varphi r - t_0], 0\} \quad (24)$$

Similarly, the number of holding vehicles at $t = T_C + T^* - (k-j-1)C - \varphi r$, denoted as $R_{2,1,j+1}$, $\forall j = 1, 2, \dots, k-1$ can be estimated as follows:

$$R_{2,1,j+1} = \max\{R_{2,1,j} + \bar{q}_N C - sg, 0\}. \quad (25)$$

Thus, $R_{2,1}$ can be estimated as follows:

$$R_{2,1} = \max\{R_{2,1,k} + \bar{q}_N [T_1^{(2)} - (T_C - \varphi r)], 0\} + 1. \quad (26)$$

By taking into account [Axiom 1](#), the estimation of $R_{2,1}$ can be refined to

$$R_{2,1} = \min\left\{\max\{R_{2,1,k} + \bar{q}_N [T_1^{(2)} - (T_C - \varphi r)], 0\}, \frac{l - L_1^{(2)}}{l_e}\right\} + 1. \quad (27)$$

The second component, $R_{2,2}$, represents the number of holding vehicles between the first and second moving holding CVs, including the second moving holding CV; the third component, $R_{2,3}$, represents the number of holding vehicles between the second and third moving holding CVs, including the third moving holding CV, and so forth. The $(k_2 + 1)^{th}$ component, R_{2,k_2+1} , represents the number of holding vehicles after the last moving holding CV. $R_{2,j}$, $\forall j = 2, 3, \dots, k_2 + 1$ is fully consistent with Eqs. [\(18\)](#) and [\(19\)](#). Thus, it follows that

$$R_2 = \min\left\{\max\{R_{2,1,k} + \bar{q}_N [T_1^{(2)} - (T_C - \varphi r)], 0\}, \frac{l - L_1^{(2)}}{l_e}\right\} + \sum_{j=2}^{k_2} \min\left\{\bar{q}_N (T_j^{(2)} - T_{j-1}^{(2)}), \frac{L_{j-1}^{(2)} - L_j^{(2)}}{l_e} - 1\right\} + \bar{q}_N (T_C - T_{k_2}^{(2)}) + k_2, \quad (28)$$

where $k = \lceil (T_C + T^* - t_0)/C \rceil$ and

$$R_{2,1,j+1} = \begin{cases} \max\{[T_C - (k-1)C - \varphi r - T_0] \bar{q}_N - s[T_C + T^* - (k-1)C - \varphi r - t_0], 0\}, & j = 0 \\ \max\{R_{2,1,j} + \bar{q}_N C - sg, 0\}, & j > 0 \end{cases}. \quad (29)$$

As $R_1 = 0$ and based on Eq. [\(12\)](#), Eq. [\(22\)](#) is obtained. Q.E.D.

Proposition 4. As $V^{(1)} = \emptyset$ and $V^{(2)} = \emptyset$ in a lane at an instant falling within the effective red of a signal group, the number of holding vehicles in this lane at this instant, R , can be estimated as follows:

$$R = \begin{cases} \min\left\{R_2, \max\left\{\frac{l - L_1}{l_e} - \bar{q}(1 - \bar{p})(T_1 - T_C), 0\right\}\right\}, & \text{if } L_1 \text{ and } T_1 \text{ exist} \\ R_2, & \text{otherwise} \end{cases}, \quad (30)$$

where L_1 is the location of the first new CV at this instant, and T_1 is the entry time of the first new CV at this instant. R_2 is determined as follows:

$$R_2 = \max\{R_{2,1,k} + \bar{q}(1 - \bar{p})\varphi r, 0\}, \quad (31)$$

where $R_{2,1,k}$ is obtained from Eq. [\(29\)](#), and $k = \lceil (T_C + T^* - t_0)/C \rceil$.

Proof. $V^{(1)} = \emptyset$ and $V^{(2)} = \emptyset$, which indicates that there is no holding CV at the instant of interest. However, holding NCs may still exist. To estimate the number of holding vehicles, multiple cycles are considered using the information of the last discharged CV (e.g., Vehicle 6 in [Fig. 2\(a\)](#)). The estimation involves the first k cycles, which are consistent with Eqs. [\(24\)](#) and [\(25\)](#). Thus, the number of holding vehicles at $t = T_C + T^*$, denoted as R_2 , can be derived as follows:

$$R_2 = \max\{R_{2,1,k} + \bar{q}_N \varphi r, 0\}, \quad (32)$$

where $R_{2,1,k}$ is obtained based on Eq. [\(29\)](#) and $k = \lceil (T_C + T^* - t_0)/C \rceil$.

If there are new CVs at the instant of interest, the upper bound of the number of holding vehicles can be deduced. Let L_1 be the location of the first new CV at $t = T_C + T^*$ and T_1 be the entry time of the first CV at the instant of interest. Then, the maximum number of holding vehicles, R_{max} , can be estimated as follows:

$$R_{max} = \max\left\{\frac{l - L_1}{l_e} - \bar{q}_N (T_1 - T_C), 0\right\}. \quad (33)$$

Thus,

$$R = \begin{cases} \min\{R_2, R_{max}\}, & \text{if } L_1 \text{ and } T_1 \text{ exist} \\ R_2, & \text{otherwise} \end{cases}. \quad (34)$$

Substituting Eqs. (12), (32), and (33) into Eq. (34) affords Eq. (30). Q.E.D.

Consequently, the CVHV-I sub-model is established as follows. The number of holding vehicles can be continuously estimated by setting different values of φ .

$$R = \begin{cases} \textbf{Proposition 1, if } V^{(1)} \neq \emptyset \text{ and } V^{(2)} = \emptyset \\ \textbf{Proposition 2, if } V^{(1)} \neq \emptyset \text{ and } V^{(2)} \neq \emptyset \\ \textbf{Proposition 3, if } V^{(1)} = \emptyset \text{ and } V^{(2)} \neq \emptyset \\ \textbf{Proposition 4, if } V^{(1)} = \emptyset \text{ and } V^{(2)} = \emptyset \end{cases}. \quad (35)$$

3.3. CVHV-II sub-model

This subsection details the CVHV-II sub-model that estimates the number of holding vehicles at an instant of interest falling within the effective green period of a signal group. The holding vehicle patterns in this situation can be more complex than those in Section 3.2, mainly due to the incomplete discharge caused by short green periods. Accordingly, a set of analytical models **Propositions 5–10** is derived to capture distinct holding vehicle patterns.

Proposition 5. Given that $V^{(1)} \neq \emptyset$, $V^{(2,1)} = \emptyset$, and $V^{(2,2)} = \emptyset$ in a lane at an instant falling within the effective green of a signal group, the number of holding vehicles in this lane at this instant, R , can be estimated as follows:

$$R = \max\left\{\frac{l - L_{k_1}^{(1)}}{l_e} + 1 - s\theta g, 0\right\} + \bar{q}(1 - \bar{p})(T_C - T_{k_1}^{(1)}). \quad (36)$$

Proof. $V^{(1)} \neq \emptyset$ indicates the presence of stopped holding CVs. $V^{(2,1)} = \emptyset$ indicates that there are no moving holding CVs before the stopped holding CVs, but there may be moving NCs. $V^{(2,2)} = \emptyset$ implies the absence of moving holding CVs after the stopped holding CVs. The maximum number of vehicles before the last stopped holding CV, denoted as R'_1 , can be estimated using the average effective vehicle length, as follows:

$$R'_1 = \frac{l - L_{k_1}^{(1)}}{l_e} + 1, \quad (37)$$

where l , $L_{k_1}^{(1)}$, and l_e represent the link length, the location of $V_{k_1}^{(1)}$ measured from the upstream intersection to the front bumper of $V_{k_1}^{(1)}$, and the average effective vehicle length, respectively. However, it is expected that some vehicles in R'_1 are discharged during green phase of θg . Therefore, the expected number of discharged vehicles, denoted as R''_1 , is estimated based on the saturation flow rate, as follows:

$$R''_1 = s\theta g, \quad (38)$$

where s represents the saturation flow rate. Thus, R_1 is given by

$$R_1 = \max\{R'_1 - R''_1, 0\} = \max\left\{\frac{l - L_{k_1}^{(1)}}{l_e} + 1 - s\theta g, 0\right\}. \quad (39)$$

The maximum operator in Eq. (39) guarantees that the estimate will always be non-negative. R_2 is consistent with Eq. (11). Thus,

$$R = \max\left\{\frac{l - L_{k_1}^{(1)}}{l_e} + 1 - s\theta g, 0\right\} + \bar{q}_N(T_C - T_{k_1}^{(1)}). \quad (40)$$

Substituting Eq. (12) into Eq. (40) affords Eq. (36). Q.E.D.

Proposition 6. Given that $V^{(1)} \neq \emptyset$, $V^{(2,1)} = \emptyset$, and $V^{(2,2)} \neq \emptyset$ in a lane at an instant falling within the effective green of a signal group, the number of holding vehicles in this lane at this instant, R , can be estimated as follows:

$$R = \max\left\{\frac{l - L_{k_1}^{(1)}}{l_e} + 1 - s\theta g, 0\right\} + \min\left\{\bar{q}(1 - \bar{p})(T_1^{(2)} - T_{k_1}^{(1)}), \frac{L_{k_1}^{(1)} - L_1^{(2)}}{l_e} - 1\right\} + B_2^{k_2} + E + k_2. \quad (41)$$

Proof. As $V^{(1)} \neq \emptyset$ and $V^{(2,1)} = \emptyset$, R_1 is fully consistent with Eq. (39). As $V^{(2,2)} \neq \emptyset$, multiple components have to be considered for R_2 . First, the number of holding vehicles between $V_{k_1}^{(1)}$ and $V_{m+1}^{(2)}$, including $V_{m+1}^{(2)}$, denoted as $R_{2,1}$, can be estimated as follows:

$$R_{2,1} = \bar{q}_N(T_{m+1}^{(2)} - T_{k_1}^{(1)}) + 1. \quad (42)$$

Given the physical size constraint stated in [Axiom 1](#),

$$R_{2,1} = \min \left\{ \bar{q}_N \left(T_{m+1}^{(2)} - T_{k_1}^{(1)} \right), \frac{L_{k_1}^{(1)} - L_{m+1}^{(2)}}{l_e} - 1 \right\} + 1. \quad (43)$$

Similarly, the number of holding vehicles between $V_{m+j-1}^{(2)}$ and $V_{m+j}^{(2)}$, including $V_{m+j}^{(2)}$, denoted $R_{2,j}$, $\forall j = 2, 3, \dots, k_2 - m$ can be estimated as follows:

$$R_{2,j} = \min \left\{ \bar{q}_N \left(T_{m+j}^{(2)} - T_{m+j-1}^{(2)} \right), \frac{L_{m+j-1}^{(2)} - L_{m+j}^{(2)}}{l_e} - 1 \right\} + 1. \quad (44)$$

Finally, the number of holding vehicles after $V_{k_2}^{(2)}$, denoted as R_{2,k_2-m+1} , can be estimated as follows:

$$R_{2,k_2-m+1} = \bar{q}_N \left(T_C - T_{k_2}^{(2)} \right). \quad (45)$$

Thus,

$$\begin{aligned} R_2 &= \sum_{j=1}^{k_2-m+1} R_{2,j} \\ &= \min \left\{ \bar{q}_N \left(T_{m+1}^{(2)} - T_{k_1}^{(1)} \right), \frac{L_{k_1}^{(1)} - L_{m+1}^{(2)}}{l_e} - 1 \right\} + \sum_{j=2}^{k_2-m} \min \left\{ \bar{q}_N \left(T_{m+j}^{(2)} - T_{m+j-1}^{(2)} \right), \frac{L_{m+j-1}^{(2)} - L_{m+j}^{(2)}}{l_e} - 1 \right\} + \bar{q}_N \left(T_C - T_{k_2}^{(2)} \right) + k_2 - m. \end{aligned} \quad (46)$$

As $V^{(2,1)} = \emptyset$, $m = 0$. Substituting $m = 0$ and Eq. (12) into Eq. (46), and then summing Eqs. (39) and (46), affords Eq. (41). Q.E.D.

Proposition 7. Given that $V^{(1)} \neq \emptyset$, $V^{(2,1)} \neq \emptyset$, and $V^{(2,2)} = \emptyset$ in a lane at an instant falling within the effective green of a signal group, the number of holding vehicles in this lane at this instant, R , can be estimated as follows:

$$R = \min \left\{ \max \left\{ \frac{l - l_1^{(2)}}{l_e} - s\theta g, 0 \right\}, \frac{l - L_1^{(2)}}{l_e} \right\} + \frac{l_1^{(2)} - L_{k_1}^{(1)}}{l_e} + \bar{q}(1 - \bar{p}) \left(T_C - T_{k_1}^{(1)} \right) + 1. \quad (47)$$

Proof. $V^{(1)} \neq \emptyset$ implies the presence of stopped holding CVs. $V^{(2,1)} \neq \emptyset$ means that there are moving holding CVs before the stopped holding CVs. $V^{(2,2)} = \emptyset$ indicates the absence of moving holding CVs after the stopped holding CVs. Moreover, it is apparent that the vehicles between the first moving holding CV and the last stopped holding CV (e.g., vehicles 7 and 8 in Fig. 1(b)) must have been part of a constrained queue at some point. Thus, R_1 can be divided into two components: the number of holding vehicles before the first moving holding CV, denoted as $R_{1,1}$, and the number of holding vehicles between the first moving CV and the last stopped holding CV, denoted as $R_{1,2}$.

$R_{1,1}$ can be estimated as follows:

$$R_{1,1} = \max \left\{ \frac{l - l_1^{(2)}}{l_e} - s\theta g, 0 \right\}, \quad (48)$$

where $l_1^{(2)}$ represents the location at which the first moving holding CV has stopped; $\frac{l - l_1^{(2)}}{l_e}$ is the upper bound of the number of holding vehicles before the first moving holding CV; and $s\theta g$ estimates the number of discharged holding vehicles during θg . Applying the physical size constraint stated in Axiom 1 gives

$$R_{1,1} = \min \left\{ \max \left\{ \frac{l - l_1^{(2)}}{l_e} - s\theta g, 0 \right\}, \frac{l - L_1^{(2)}}{l_e} \right\}. \quad (49)$$

$R_{1,2}$ can be estimated as follows:

$$R_{1,2} = \frac{l_1^{(2)} - L_{k_1}^{(1)}}{l_e} + 1. \quad (50)$$

Thus, R_1 can be obtained as follows:

$$R_1 = R_{1,1} + R_{1,2} = \min \left\{ \max \left\{ \frac{l - l_1^{(2)}}{l_e} - s\theta g, 0 \right\}, \frac{l - L_1^{(2)}}{l_e} \right\} + \frac{l_1^{(2)} - L_{k_1}^{(1)}}{l_e} + 1. \quad (51)$$

As $V^{(2,2)} = \emptyset$, R_2 is consistent with Eq. (11). Substituting Eq. (12) into the summation of R_1 and R_2 gives Eq. (47). Q.E.D.

Proposition 8. As $V^{(1)} \neq \emptyset$, $V^{(2,1)} \neq \emptyset$, and $V^{(2,2)} \neq \emptyset$ in a lane at an instant falling within the effective green of a signal group, the number of holding vehicles in this lane at this instant, R , can be estimated as follows:

$$R = \min \left\{ \max \left\{ \frac{l - l_1^{(2)}}{l_e} - s\theta g, 0 \right\}, \frac{l - L_1^{(2)}}{l_e} \right\} + \frac{l_1^{(2)} - L_{k_1}^{(1)} + l_e(1 + B_2^{k_2-m} + E + k_2 - m)}{l_e} + \min \left\{ \bar{q}(1 - \bar{p})(T_{m+1}^{(2)} - T_{k_1}^{(1)}), \frac{L_{k_1}^{(1)} - L_{m+1}^{(2)}}{l_e} - 1 \right\}. \quad (52)$$

Proof. As $V^{(1)} \neq \emptyset$ and $V^{(2,1)} \neq \emptyset$, R_1 is fully consistent with that in [Proposition 7](#). Similarly, R_2 follows the same form as in [Proposition 6](#), with the only difference being that $m \neq 0$. Therefore, the proof is automatically completed, relying on the proofs provided for [Propositions 6 and 7](#). Q.E.D.

Proposition 9. As $V^{(1)} = \emptyset$ and $V^{(2)} \neq \emptyset$ in a lane at an instant falling within the effective green of a signal group, the number of holding vehicles in this lane at this instant, R , can be estimated as follows:

$$R = \begin{cases} \min \left\{ A, \frac{l - L_1^{(2)}}{l_e} + 1 \right\} + B_2^{k_2} + E + k_2 - 1, & \text{if } F = 0 \\ \min \left\{ A, \frac{l - L_1^{(2)}}{l_e} + 1 \right\} + \frac{l_1^{(2)} - l_2^{(2)}}{l_e} + B_{z+1}^{k_2} + E + k_2 - z, & \text{if } F = 1 \end{cases}, \quad (53)$$

where $A = R_{2,1,k}$ if $t_0 \geq T_C + T^* - \theta g - (k - 1)C$ and

$$R_{2,1,j} = \begin{cases} \max \left\{ \bar{q}_N(T_1^{(2)} - T_0) - s(T_C + T^* - t_0), 0 \right\} + 1, & j = 1 \\ \max \{R_{2,1,j-1} + \bar{q}_N C - sg, 0\}, & 1 < j \leq k - 1 \\ \max \{R_{2,1,j-1} + \bar{q}_N [T_1^{(2)} - (T_C - r - \theta g)] - s\theta g, 0\} + 1, & j = k \end{cases}; \quad (54)$$

otherwise, $A = R_{2,1,k+1}$ and

$$R_{2,1,j} = \begin{cases} \max \{[T_C - kC + (1 - \theta)g - T_0]\bar{q}_N - s[T_C + T^* - kC + (1 - \theta)g - t_0], 0\}, & j = 1 \\ \max \{R_{2,1,j-1} + \bar{q}_N C - sg, 0\}, & 1 < j \leq k \\ \max \{R_{2,1,j-1} + \bar{q}_N [T_1^{(2)} - (T_C - r - \theta g)] - s\theta g, 0\} + 1, & j = k + 1 \end{cases}; \quad (55)$$

$F = 0$ indicates that none of the vehicles in $V^{(2)}$ stops in time interval $[T_C + T^* - C, T_C + T^*]$. Otherwise, $F = 1$; $\bar{q}_N = \bar{q}(1 - \bar{p})$; and $k = \lceil (T_C + T^* - t_0)/C \rceil$.

Proof. As $V^{(1)} = \emptyset$, $R_1 = 0$. $V^{(2)} \neq \emptyset$ indicates that there is at least one moving holding CV. Multiple holding components have to be considered. The first component is the number of holding vehicles before the first moving holding CV, denoted as $R_{2,1}$. Let $k = \lceil (T_C + T^* - t_0)/C \rceil$ represent the number of cycles involved in estimating $R_{2,1}$. Thus, $R_{2,1}$ has the following possible expressions:

If $t_0 \geq T_C + T^* - \theta g - (k - 1)C$ and $k = 1$,

$$R_{2,1} = R_{2,1,1} = \max \left\{ \bar{q}_N(T_1^{(2)} - T_0) - s(T_C + T^* - t_0), 0 \right\} + 1. \quad (56)$$

If $t_0 \geq T_C + T^* - \theta g - (k - 1)C$ and $k > 1$, multiple cycles have to be considered. If $t \in [t_0, T_C + T^* - (k - 1)C + (1 - \theta)g]$, the number of holding vehicles in this period, denoted as $R_{2,1,1}$, can be estimated as follows:

$$R_{2,1,1} = \max \{[T_C - (k - 1)C + (1 - \theta)g - T_0]\bar{q}_N - s[T_C + T^* - (k - 1)C + (1 - \theta)g - t_0], 0\}, \quad (57)$$

Similarly, if $t \in [T_C + T^* - (k - j + 1)C + (1 - \theta)g, T_C + T^* - (k - j)C + (1 - \theta)g]$, $R_{2,1,j}$, $\forall j = 2, 3, \dots, k - 1$, can be estimated as follows:

$$R_{2,1,j} = \max \{R_{2,1,j-1} + \bar{q}_N C - sg, 0\}. \quad (58)$$

The last time interval $t \in [T_C + T^* - C + (1 - \theta)g, T_C + T^*]$ affords

$$R_{2,1,k} = \max \{R_{2,1,k-1} + \bar{q}_N [T_1^{(2)} - (T_C - r - \theta g)] - s\theta g, 0\} + 1. \quad (59)$$

Using [Axiom 1](#),

$$R_{2,1} = \min \left\{ R_{2,1,k}, \frac{l - L_1^{(2)}}{l_e} + 1 \right\}. \quad (60)$$

Similarly, if $t_0 < T_C + T^* - \theta g - (k - 1)C$, multiple cycles have to be considered. If $t \in [t_0, T_C + T^* - kC + (1 - \theta)g]$, the number of holding vehicles in this period, denoted as $R_{2,1,1}$, can be estimated as follows:

$$R_{2,1,1} = \max\{[T_C - kC + (1 - \theta)g - T_0]\bar{q}_N - s[T_C + T^* - kC + (1 - \theta)g - t_0], 0\}. \quad (61)$$

Similarly, if $t \in [T_C + T^* - (k - j + 2)C + (1 - \theta)g, T_C + T^* - (k - j + 1)C + (1 - \theta)g]$, $R_{2,1,j}$, $\forall j = 2, 3, \dots, k - 1$, can be estimated as follows:

$$R_{2,1,j} = \max\{R_{2,1,j-1} + \bar{q}_N C - sg, 0\}, j = 2, 3, \dots, k. \quad (62)$$

The last time interval $t \in [T_C + T^* - C + (1 - \theta)g, T_C + T^*]$ affords

$$R_{2,1,k+1} = \max\{R_{2,1,k} + \bar{q}_N \left[T_1^{(2)} - (T_C - r - \theta g) \right] - s\theta g, 0\} + 1. \quad (63)$$

Using [Axiom 1](#),

$$R_{2,1} = \min\left\{ R_{2,1,k+1}, \frac{l - L_1^{(2)}}{l_e} + 1 \right\}. \quad (64)$$

Now, consider the holding components after the first moving holding CV. If none of the vehicles in $V^{(2)}$ stops in time interval $[T_C + T^* - C, T_C + T^*]$, the number of holding vehicles between $V_{j-1}^{(2)}$ and $V_j^{(2)}$, denoted as $R_{2,j}$, $\forall j = 2, 3, \dots, k_2 + 1$, is fully consistent with Eqs. [\(18\)](#) and [\(19\)](#). Thus,

$$R_2 = R_{2,1} + \sum_{j=2}^{k_2} \min\left\{ \bar{q}_N \left(T_j^{(2)} - T_{j-1}^{(2)} \right), \frac{L_{j-1}^{(2)} - L_j^{(2)}}{l_e} - 1 \right\} + \bar{q}_N \left(T_C - T_{k_2}^{(2)} \right) + k_2 - 1. \quad (65)$$

In contrast, if some vehicles in $V^{(2)}$ stop at the red signal in time interval $[T_C + T^* - C, T_C + T^*]$, the stopping locations of $V_j^{(2)}$ are denoted as $l_j^{(2)}$, $\forall j = 1, 2, \dots, z$. The number of holding vehicles between $V_1^{(2)}$ and $V_z^{(2)}$, including $V_z^{(2)}$, can be estimated based on the average effective vehicle length, i.e., the second term in Eq. [\(66\)](#). The number of holding vehicles after $V_z^{(2)}$ can be derived based on the same method described in Eqs. [\(18\)](#) and [\(19\)](#) but starting with $V_{z+1}^{(2)}$. Thus, R_2 can be obtained as follows:

$$R_2 = R_{2,1} + \frac{l_1^{(2)} - l_z^{(2)}}{l_e} + \sum_{j=z+1}^{k_2} \min\left\{ \bar{q}_N \left(T_j^{(2)} - T_{j-1}^{(2)} \right), \frac{L_{j-1}^{(2)} - L_j^{(2)}}{l_e} - 1 \right\} + \bar{q}_N \left(T_C - T_{k_2}^{(2)} \right) + k_2 - z. \quad (66)$$

Substituting Eqs. [\(12\)](#), [\(60\)](#), and [\(64\)](#) into Eqs. [\(65\)](#) and [\(66\)](#) furnishes Eq. [\(53\)](#). Q.E.D.

Proposition 10. As $V^{(1)} = \emptyset$ and $V^{(2)} = \emptyset$ in a lane at an instant falling within the effective green of a signal group, the number of holding vehicles in this lane at this instant, R , can be estimated as follows:

$$R = \begin{cases} \min\left\{ R_{2,1}, \max\left\{ \frac{l - L_1}{l_e} - \bar{q}_N(T_1 - T_C), 0 \right\} \right\}, & \text{if } L_1 \text{ and } T_1 \text{ exist} \\ R_{2,1}, & \text{otherwise} \end{cases}, \quad (67)$$

where $R_{2,1} = R_{2,1,k}$ if $t_0 \geq T_C + T^* - \theta g - (k - 1)C$ and

$$R_{2,1,j} = \begin{cases} \max\left\{ \bar{q}_N \left(T_1^{(2)} - T_0 \right) - s(T_C + T^* - t_0), 0 \right\} + 1, & j = 1 \\ \max\{R_{2,1,j-1} + \bar{q}_N C - sg, 0\}, & 1 < j \leq k - 1 \\ \max\{R_{2,1,j-1} + \bar{q}_N(r + \theta g) - s\theta g, 0\}, & j = k \end{cases}, \quad (68)$$

otherwise, $R_{2,1} = R_{2,1,k+1}$ and

$$R_{2,1,j} = \begin{cases} \max\{[T_C - kC + (1 - \theta)g - T_0]\bar{q}_N - s[T_C + T^* - kC + (1 - \theta)g - t_0], 0\}, & j = 1 \\ \max\{R_{2,1,j-1} + \bar{q}_N C - sg, 0\}, & 1 < j \leq k \\ \max\{R_{2,1,j-1} + \bar{q}_N(r + \theta g) - s\theta g, 0\}, & j = k + 1 \end{cases}; \quad (69)$$

$\bar{q}_N = \bar{q}(1 - \bar{p})$; and $k = \lceil (T_C + T^* - t_0)/C \rceil$.

Proof. $V^{(1)} = \emptyset$ and $V^{(2)} = \emptyset$, which indicates that there are no holding CVs but there may be holding NCs. Let $k = \lceil (T_C + T^* - t_0^{(2)})/C \rceil$ represent the number of cycles involved in estimating $R_{2,1}$, which here represents the number of holding vehicles at the instant of interest. Consequently, the following possibilities exist.

If $t_0 \geq T_C + T^* - \theta g - (k - 1)C$ and $k = 1$,

$$R_{2,1} = R_{2,1,1} = \max\{\bar{q}_N(T_C - T_0) - s(T_C + T^* - t_0), 0\}. \quad (70)$$

If $t_0 \geq T_C + T^* - \theta g - (k - 1)C$ and $k > 1$, $R_{2,1,j}$, $\forall j = 1, 2, \dots, k - 1$ are fully consistent with the associated expressions stated in

Proposition 9. $R_{2,1,k}$ is derived as follows:

$$R_{2,1} = R_{2,1,k} = \max\{R_{2,1,k-1} + \bar{q}_N(r + \theta g) - s\theta g, 0\}. \quad (71)$$

If $t_0 < T_C + T^* - \theta g - (k-1)C$, $R_{2,1,j}$, $\forall j = 1, 2, \dots, k$ are also fully consistent with the associated expressions stated in [Proposition 9](#). $R_{2,1,k+1}$ is given by

$$R_{2,1} = R_{2,1,k+1} = \max\{R_{2,1,k} + \bar{q}_N(r + \theta g) - s\theta g, 0\}. \quad (72)$$

Finally, if there are new CVs at the instant of interest, the upper bound of the number of holding vehicles can be deduced. Let L_1 be the location of the first new CV at $t = T_C + T^*$, and let T_1 be the entry time of the first new CV at $t = T_C + T^*$. Then, the maximum number of holding vehicles, R_{max} , can be estimated as follows:

$$R_{max} = \max\left\{\frac{l - L_1}{l_e} - \bar{q}_N(T_1 - T_C), 0\right\}. \quad (73)$$

Thus,

$$R = \begin{cases} \min\{R_{2,1}, R_{max}\}, & \text{if } L_1 \text{ and } T_1 \text{ exist} \\ R_{2,1}, & \text{otherwise} \end{cases}. \quad (74)$$

Substituting Eqs. (12) and (70) to (73) into Eq. (74) affords Eq. (67). Q.E.D.

Therefore, the CVHV-II sub-model is established as follows. The number of holding vehicles can be continuously estimated by setting different values of θ .

$$R = \begin{cases} \text{Proposition 5, if } V^{(1)} \neq \emptyset, V^{(2,1)} = \emptyset, \text{ and } V^{(2,2)} = \emptyset \\ \text{Proposition 6, if } V^{(1)} \neq \emptyset, V^{(2,1)} = \emptyset, \text{ and } V^{(2,2)} \neq \emptyset \\ \text{Proposition 7, if } V^{(1)} \neq \emptyset, V^{(2,1)} \neq \emptyset, \text{ and } V^{(2,2)} = \emptyset \\ \text{Proposition 8, if } V^{(1)} \neq \emptyset, V^{(2,1)} \neq \emptyset, \text{ and } V^{(2,2)} \neq \emptyset \\ \text{Proposition 9, if } V^{(1)} = \emptyset \text{ and } V^{(2)} \neq \emptyset \\ \text{Proposition 10, if } V^{(1)} = \emptyset \text{ and } V^{(2)} = \emptyset \end{cases}. \quad (75)$$

4. Numerical experiment

To validate the effectiveness of the devised models in estimating the number of holding vehicles, extensive simulation experiments were conducted using the VISSIM platform.

4.1. General settings

A 1-km link connected to a signalized intersection was considered. Vehicle arrivals followed a Poisson process, and all of the vehicles were cars. The simulation resolution was set to 0.1 s, meaning that vehicle states were updated every 0.1 s. The saturation flow rate and average effective vehicle length were determined based on observations from multiple runs, resulting in values of 0.63 veh/s and 6.44 m, respectively. The signal timings consisted of red, green, and amber phases, with a fixed amber duration of 3 s following the green phase. The cycle length was set to 60 s. All of the other parameters were set as default values in VISSIM. Vehicle identities were randomly assigned according to the preset CV penetration rate, π , where the probabilities of being a CV and an NC were represented by π and $1 - \pi$, respectively. With the advancements in 5G communication technologies, which provide a latency as low as 0.01 s ([Tahir and Katz 2022](#)), CV data can be accessed in real-time. Simulations were conducted under various combinations of V/C values, signal timings, CV penetration rates, and instants of interest to represent different cases. Each case comprised 1,000 simulation cycles. The actual number of holding vehicles in each cycle, R_{GT} , served as the ground truth and was recorded for evaluation purposes.

4.2. Holding vehicle estimation

The actual traffic demands and CV penetration rates were unknown during the estimation of the number of holding vehicles. For illustrative purposes, the efficient CDT model was used in MLE for estimating \bar{q} and \bar{p} . The CVHV model was applied (with the CVHV-I sub-model for the instant of interest falling within the effective red of a signal group and the CVHV-II sub-model for the instant of interest falling within the effective green of a signal group), utilizing only the available CV information, to estimate the number of holding vehicles, \hat{R} .

To the best of available knowledge, no existing method systematically estimates the number of holding vehicles in a controlling lane at any instant of interest. However, [Jia et al. \(2024a, 2024b\)](#) proposed a residual-vehicle (RV) model to estimate the holding vehicle distribution at the end of effective greens. The mean of the real-time residual-vehicle distribution can be used as the estimate for the number of holding vehicles in a specific lane at the end of effective green. Also, the sum of this estimated number of holding vehicles at the end of effective green and the expected number of arrivals during the subsequent red period can estimate the number of holding vehicles in a lane at an instant of interest falling within the effective red of a signal group. Thus, the RV model can estimate the number of holding vehicles in lanes at the instant of interest falling within the effective red or at the end of effective green of a signal

group. Nevertheless, the RV model cannot estimate the number of holding vehicles in lanes at the instant of interest falling within the effective green of a signal group. Further details can be found in Jia et al. (2024a, 2024b). Despite this limitation, the RV model was employed to provide valuable benchmarks for holding vehicle estimation, even though only partial cases could be evaluated using it. Additionally, a simple and generic scaling method, widely applied in estimating various traffic state quantities such as traffic demand, traffic volume, and queue length (Zhao et al., 2019b), was adopted as an alternative benchmark. This method estimates the number of holding vehicles by dividing the number of holding CVs by the CV penetration rate, ρ . To assess the full capability of the scaling method, the true CV penetration rate, ρ , was utilized in all experiments. However, it is important to note that ρ is treated as unknown in the proposed CVHV model.

The root-mean-square error (RMSE), mean absolute error (MAE), and the variance of difference (VoD) (i.e., $Var(R_{GT} - \hat{R})$ here) were the chosen performance metrics evaluating the estimation accuracy and efficiency of the models.

4.3. Results

Table 2 summarizes the performance of the CVHV-I sub-model in estimating the number of holding vehicles at the instant of interest falling within the effective red of a signal group. For the baseline case with $r = 30$, $V/C = 0.5$, $p = 0.4$, and $\varphi = 0.5$, the RMSE and MAE for the CVHV-I sub-model were 0.88 and 0.65, respectively, compared to 1.77 and 1.44 for the RV model and 1.73 and 1.31 for the scaling method. The VoD for the CVHV-I sub-model in the baseline case was remarkably close to 0, i.e., 0.77, indicating efficient estimation throughout the 1,000 cycles. In contrast, the VoDs for the RV model and the scaling method were 2.37 and 3.01, respectively, signifying a significant efficiency improvement with the proposed CVHV-I sub-model.

A sensitivity analysis was devised and performed under various signal timings (Group A), V/C values (Group B), CV penetration rates (Group C), and instants of interest (Group D). Comparing the results of Group A cases with that of the baseline case shows that the performance metrics remained relatively stable, indicating that different signal timings did not have a substantial impact on the estimates of the numbers of holding vehicles. Group B cases considered various V/C values. Compared with a lower V/C value, a higher V/C value would lead to a larger number of holding vehicles, which should naturally result in slightly higher values for the performance metrics. Nevertheless, even at a near-capacity V/C value of 0.95, where the holding vehicles became substantial, the average difference was only 1.2 vehicles for the CVHV-I sub-model compared to 3.9 and 2.5 vehicles for the RV model and the scaling method. Group C cases investigated the influence of CV penetration rates on the model performance. The results revealed that the performance improved for all methods as the CV penetration rates increased. Group D examined a different instant of interest: φ was changed from 0.5 to 1.0, which represented an extreme case of the end of effective red. As φ increased, the holding vehicles became more pronounced, leading to larger values for the performance metrics. Nevertheless, the average error for the CVHV-I sub-model remained below 1 vehicle, whereas the RV model and the scaling method exhibited average errors of approximately 2 vehicles.

Fig. 3 further validates the high estimation accuracy and minimal systematic errors of the CVHV-I sub-model for all of the cases presented in **Table 2**, as indicated by the well-distributed points along the 45-degree lines. Overall, the CVHV-I sub-model consistently demonstrated significant improvements over both the RV model and the scaling method across all cases. These results confirm that the CVHV-I sub-model accurately monitors the numbers of holding vehicles under various traffic conditions and signal timings.

Table 3 presents the performance of the CVHV-II sub-model in estimating the number of holding vehicles at the instant of interest falling within the effective green of a signal group. As the RV model can only estimate the number of holding vehicles at the instant of interest falling within the effective red or at the end of effective green of a signal group, it cannot be applied for cases with $\theta = 0.5$. In general, compared with a shorter effective green, a longer effective green allowed for the discharge of more vehicles, resulting in fewer holding vehicles and a smaller error, as evident in the Groups A and D cases. The Groups B and C cases exhibited error patterns that were similar to those in **Table 2**. Comparisons between the RV model, the scaling method, and the proposed CVHV-II sub-model highlight the superior estimation accuracy of the proposed CVHV-II sub-model.

Fig. 4 illustrates the estimation accuracy of the CVHV-II sub-model in these cases. The results clearly demonstrate the capability of the CVHV-II sub-model to accurately estimate the number of holding vehicles at the instant of interest falling within the effective green of a signal group, as indicated by the tightly scattered errors and the alignment of the points along the 45-degree lines.

In real-world scenarios, intersections typically have multiple traffic streams controlled by different signal groups. The instant of interest can fall within either the effective red or effective green of a signal group. The CVHV-I and CVHV-II sub-models can be

Table 2
Performance of the CVHV-I sub-model in estimating the number of holding vehicles.

Case	r	V/C	ρ	φ	RMSE			MAE			VoD		
					RV	Scaling method	CVHV-I	RV	Scaling method	CVHV-I	RV	Scaling method	CVHV-I
Baseline	30	0.5	0.4	0.5	1.77	1.73	0.88	1.44	1.31	0.65	2.37	3.01	0.77
A-1	15	0.5	0.4	0.5	1.63	1.38	0.84	1.35	0.95	0.54	1.86	1.91	0.69
A-2	45	0.5	0.4	0.5	1.98	1.69	0.82	1.36	1.25	0.58	3.37	2.85	0.65
B-1	30	0.3	0.4	0.5	1.36	1.29	0.73	1.12	0.88	0.53	1.40	1.67	0.51
B-2	30	0.7	0.4	0.5	2.54	2.09	1.10	1.96	1.60	0.81	4.58	4.36	1.20
B-3	30	0.95	0.4	0.5	5.45	3.30	1.71	3.86	2.51	1.21	29.4	10.91	2.73
C-1	30	0.5	0.1	0.5	1.90	4.51	1.58	1.49	2.99	1.15	3.44	20.25	2.13
C-2	30	0.5	0.7	0.5	1.75	0.94	0.58	1.40	0.69	0.40	2.27	0.89	0.32
D-1	30	0.5	0.4	1	2.41	2.61	1.39	1.89	2.04	0.98	4.88	6.82	1.66

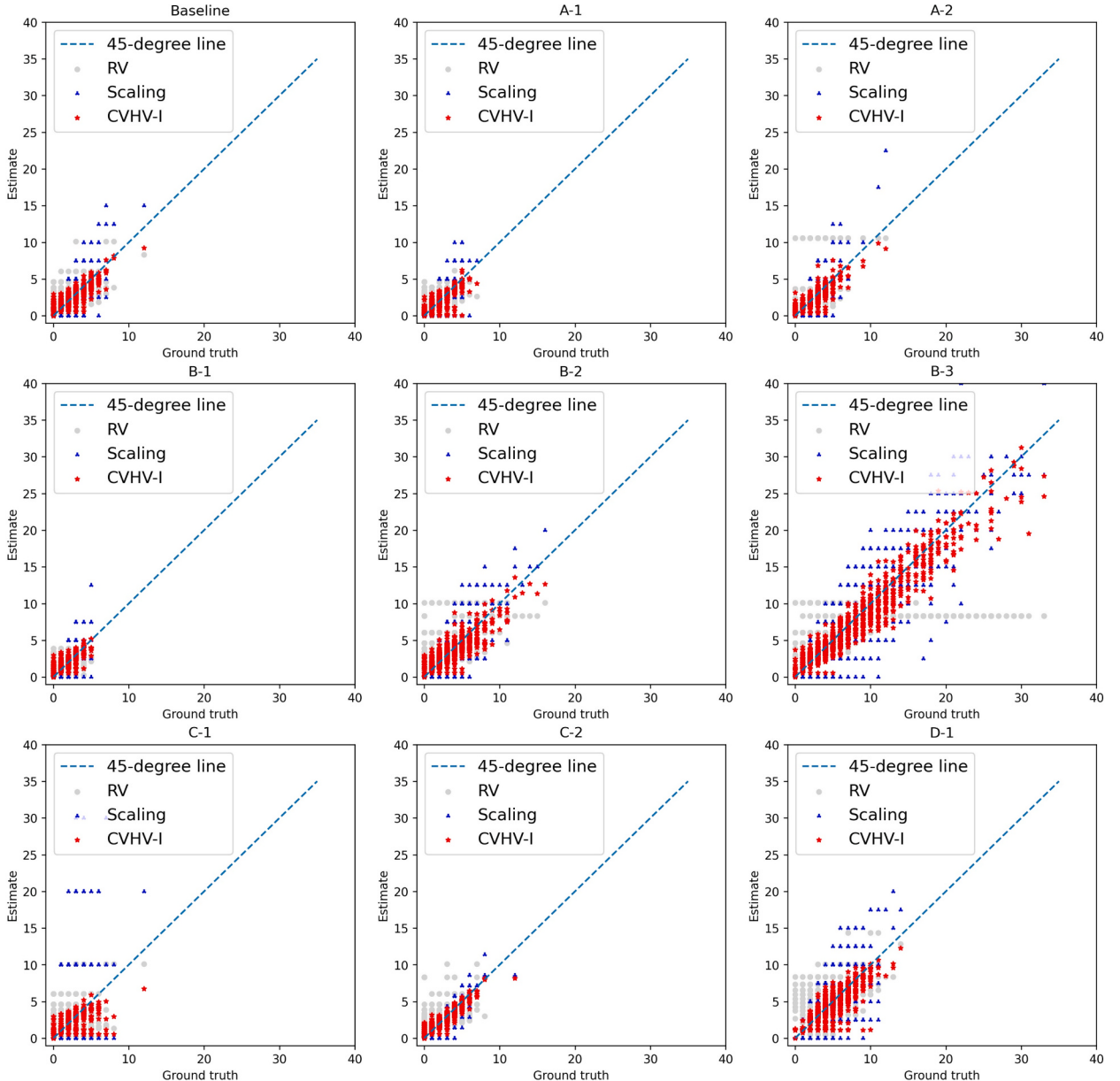


Fig. 3. Estimation accuracy of the CVHV-I sub-model.

Table 3

Performance of the CVHV-II sub-model in estimating the number of holding vehicles.

Case	r	V/C	γ	θ	RMSE		MAE		VoD				
					RV	Scaling method	CVHV-II	RV	Scaling method	CVHV-II	RV		
Baseline	30	0.5	0.4	0.5	—	1.08	0.83	—	0.54	0.40	—	1.18	0.65
A-1	15	0.5	0.4	0.5	—	0.68	0.50	—	0.24	0.16	—	0.46	0.24
A-2	45	0.5	0.4	0.5	—	1.49	1.07	—	0.94	0.65	—	2.21	0.99
B-1	30	0.3	0.4	0.5	—	0.45	0.35	—	0.13	0.09	—	0.20	0.12
B-2	30	0.7	0.4	0.5	—	2.07	1.40	—	1.40	0.91	—	4.27	1.70
B-3	30	0.95	0.4	0.5	—	3.53	1.94	—	2.56	1.41	—	12.42	3.02
C-1	30	0.5	0.1	0.5	—	2.71	1.30	—	1.16	0.69	—	7.37	1.57
C-2	30	0.5	0.7	0.5	—	0.64	0.53	—	0.31	0.24	—	0.40	0.28
D-1	30	0.5	0.4	1	0.57	0.42	0.26	0.24	0.10	0.06	0.32	0.18	0.06

seamlessly applied in such situations by selecting the appropriate model based on the instant of interest and its relationship with the signal groups. Moreover, the number of holding vehicles can be continuously monitored by adjusting the value of φ or θ . This flexible framework makes the CVHV model highly adaptable and suitable for various advanced ITS applications, including traffic state estimation and traffic signal control as demonstrated in [Section 6](#).

5. Real-world validation

The CVHV model was next applied to real-world data retrieved from the NGSIM dataset to demonstrate its practicality.

5.1. General settings

The dataset associated with the southbound through-lane between Intersections 1 and 2 on Peachtree Street in Atlanta, Georgia, USA, as shown in [Fig. 5](#), was selected. Trajectory data with a resolution of 0.1 s were collected during two time periods: 12:45–13:00 and 16:00–16:15 on November 8, 2006. The cycle lengths during these two periods were 95 s and 100 s, respectively, with red periods

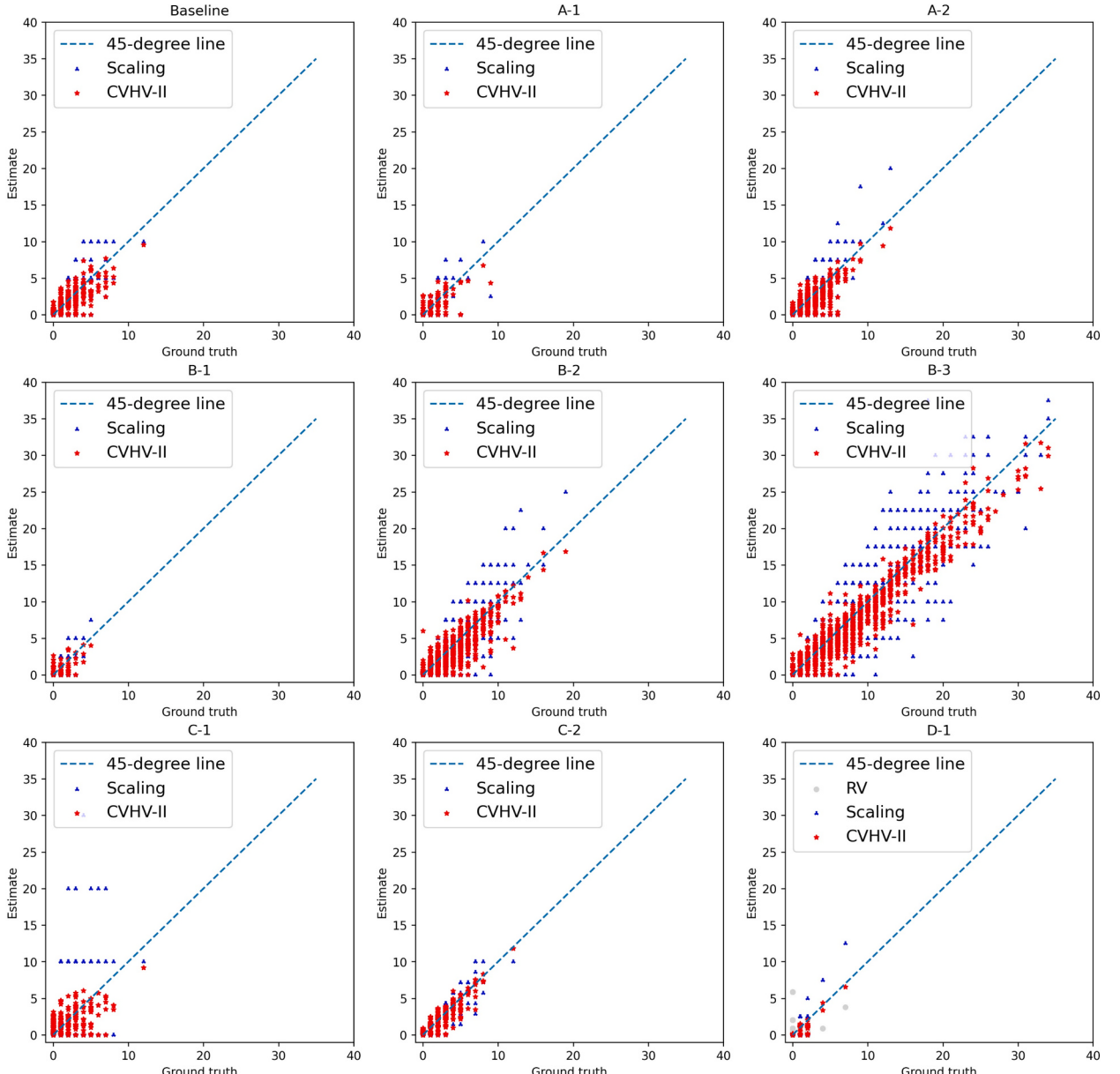


Fig. 4. Estimation accuracy of the CVHV-II sub-model.

of 62 s and 64 s, respectively. The saturation flow rate and average effective vehicle length were determined to be 0.49 veh/s and 8.47 m, respectively.

Different scenarios were devised to evaluate the performance of the CVHV model. φ and θ were set to either 0.5 or 1.0 to represent different instants of interest. To simulate different CV penetration rates, vehicles were randomly assigned to be either CVs or NCs, with CV penetration rates of 0.1, 0.4, or 0.7. The near-zero latency offered by 5G technologies enables the use of CV data in a wide range of transportation applications. The actual number of holding vehicles for each cycle, which served as the ground truth, was recorded for evaluation purposes.

5.2. Holding vehicle estimation

As each period was only 15-min long, there were only nine complete cycles in each period. The parameters \bar{q} and \bar{p} , representing the average arrival rate and CV penetration rate, respectively, were estimated based on the most recent three-cycle data. Thus, the estimation of numbers of holding vehicles was performed using data starting from the third cycle, resulting in seven estimates of the number of holding vehicles for each period. Due to the small sample size and the influence of random seeds, the estimate numbers fluctuated significantly. To mitigate this, vehicle assignment was conducted 100 times with different random seeds to afford a total of 700 estimated numbers based on the CVHV model for each period. As in the numerical experiments presented in Section 4, the RV model (Jia et al., 2024a, 2024b) and the scaling method (Zhao et al., 2019b) served as benchmark methods. The RV method was applicable only to cases where the instants of interest fell within effective red or at the end of effective green of the associated signal groups. These estimates were compared with the recorded ground truth to evaluate the estimation accuracy.

5.3. Results

Table 4 reports the numbers of holding vehicles estimated by the CVHV-I sub-model, based on the NGSIM dataset, for instants of interest falling within the effective red of the associated signal groups. The evaluation considered various CV penetration rates and

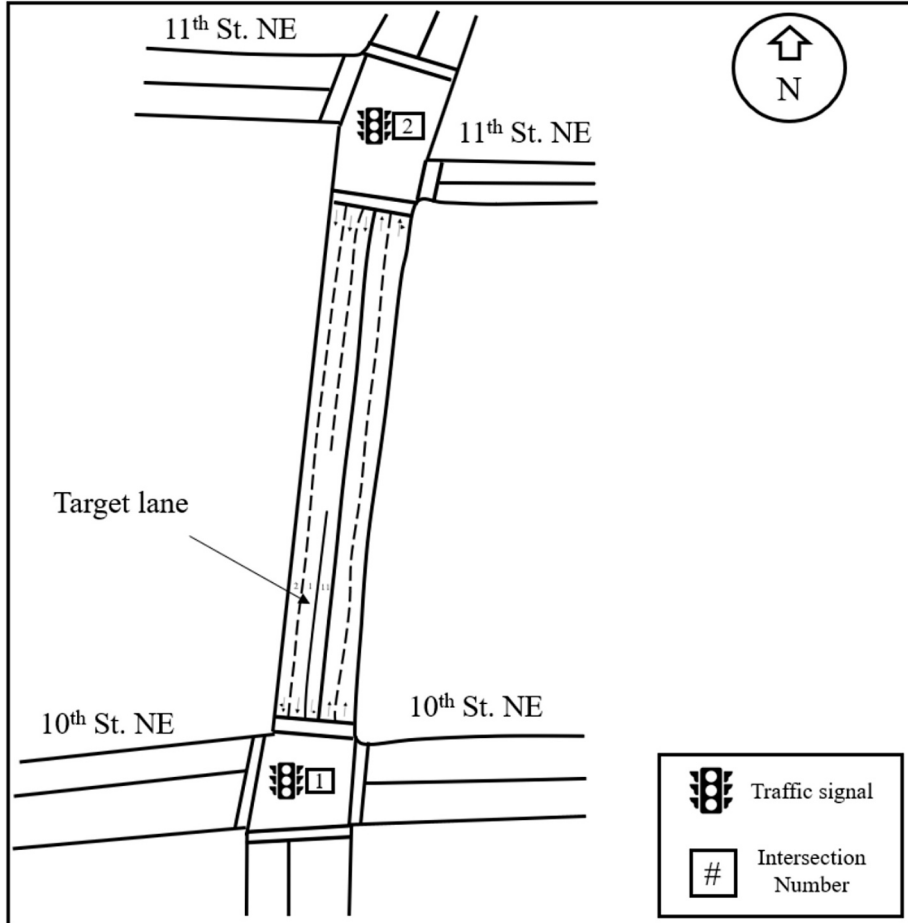


Fig. 5. Illustration of intersections 1 and 2 on Peachtree Street.

instants of interest, and the error patterns were consistent with those presented in the VISSIM simulations. In most cases, the average error was as low as one or two vehicles for the CVHV-I sub-model. Moreover, the proposed CVHV-I sub-model significantly outperformed the RV model and the scaling method.

Figs. 6 and 7 display the boxplots of the estimates, showing that the means of the estimated numbers of holding vehicles from the CVHV-I sub-model closely aligned with the ground truth values while those estimated by the RV model were far from the ground truth values. That is, despite the fluctuations of the estimates from the CVHV-I sub-model, the majority of the ground truth values fell within the ranges of the estimated numbers. In contrast, most ranges determined by the estimates from the RV model exclude the ground truth values. While the ground truths were within the range of estimates produced by the scaling method, these estimates exhibited significantly larger fluctuations compared to those from the proposed CVHV-I sub-model, especially in cases with low CV penetration rates. This further affirms the superiority of the CVHV-I sub-model. Considering the complexities of real-world traffic conditions, uncertain human driving behaviors, and the presence of unknown factors, the results demonstrate the robust performance of the CVHV-I sub-model in estimating numbers of holding vehicles.

Table 5 presents the numbers of holding vehicles estimated by the CVHV-II sub-model for instants of interest falling within the effective green of the associated signal groups, based on the NGSIM dataset. The RV model was only implemented in cases with $\theta = 1$ given its limited applicability. Due to the discharges during the green phase, the numbers of holding vehicles were generally lower than those at instants of interest falling within the effective red of the associated signal groups. The results in Table 5 show that in most cases the average error was less than one vehicle for the CVHV-II sub-model. Similar error patterns were observed to those seen in the VISSIM simulations.

Figs. 8 and 9 illustrate the estimation accuracy in the form of boxplots. Similarly, with the CVHV-II sub-model, there were only slight deviations between the mean estimated numbers and the ground truths, and the ground truths fell within the ranges of the estimated numbers. In addition, the CVHV-II sub-model was compared with the scaling method in all cases and the RV model in D-1 cases, revealing significant advancements in the CVHV-II sub-model. This further highlights the effectiveness and applicability of the CVHV-II sub-model for accurately estimating numbers of holding vehicles.

6. Applications

This section presents two example applications: the estimation of the real-time total number of vehicles in a lane and a simple illustrative example of CV-based adaptive signal control. Both applications use the estimated number of holding vehicles as an essential input, demonstrating the importance of accurately modeling holding vehicles in CV-based traffic state estimation and traffic signal control.

6.1. Estimation of real-time total number of vehicles in a lane

The total number of vehicles in a lane at an instant of interest is a critical input for the development of various ITS applications, such as max-pressure control (Varaiya, 2013) and vehicle location and speed estimation (Feng et al., 2015). One straightforward approach to estimating this number is the scaling method, as discussed in Sections 4 and 5. This method estimates the total number of vehicles in a lane at an instant of interest by dividing the number of CVs in the lane at that instant by the CV penetration rate (Zhao et al., 2019b). Because the number of CVs is known precisely, the estimation error for this method stems solely from the uncertainty in the CV penetration rate. However, the scaling method does not fully utilize the trajectory information from CVs or account for vehicle dynamics. For instance, vehicles stopped at an instant of interest that falls within the effective red of a signal group often form a queue near the stop bar. While the number of queued vehicles, forming part of the total number of vehicles in a lane, can be more accurately estimated using stopped-CV information, this is not incorporated into the scaling method. An alternative approach is the Estimation of Vehicle Location and Speed (EVLS) algorithm proposed by Feng et al. (2015). The EVLS algorithm leverages queue information and car-following behavior to estimate the total number of vehicles in a lane, as well as their precise locations and speeds. However, this algorithm tends to overestimate the total number of vehicles in a lane, primarily because it inserts additional vehicles into the slowing-down region due to dynamic car-following distances.

The real-time total number of vehicles in a lane at an instant of interest can be decomposed into new arrivals and holding vehicles. By leveraging the proposed CVHV model, which estimates the number of holding vehicles in a lane, a new method for estimating the

Table 4

Performance of the CVHV-I sub-model in estimating the number of holding vehicles based on the NGSIM dataset.

Period	Case	θ	φ	RMSE		MAE		VoD		
				RV	Scaling method	CVHV-I	RV	Scaling method	CVHV-I	CVHV-I
12:45	Baseline	0.4	0.5	2.48	2.33	1.71	2.07	1.86	1.26	2.64
	C-1	0.1	0.5	3.14	5.79	2.75	2.67	4.53	2.23	3.44
13:00	C-2	0.7	0.5	2.37	1.25	1.11	1.94	0.99	0.81	2.53
	D-1	0.4	1	1.70	2.32	1.49	1.36	1.84	1.19	2.87
16:00	Baseline	0.4	0.5	3.72	3.10	2.55	2.85	2.38	1.92	12.50
	C-1	0.1	0.5	4.28	7.80	4.18	3.55	6.24	3.25	12.99
16:15	C-2	0.7	0.5	3.55	2.00	1.86	2.77	1.64	1.38	12.10
	D-1	0.4	1	7.31	2.63	2.46	6.47	1.98	1.97	14.31

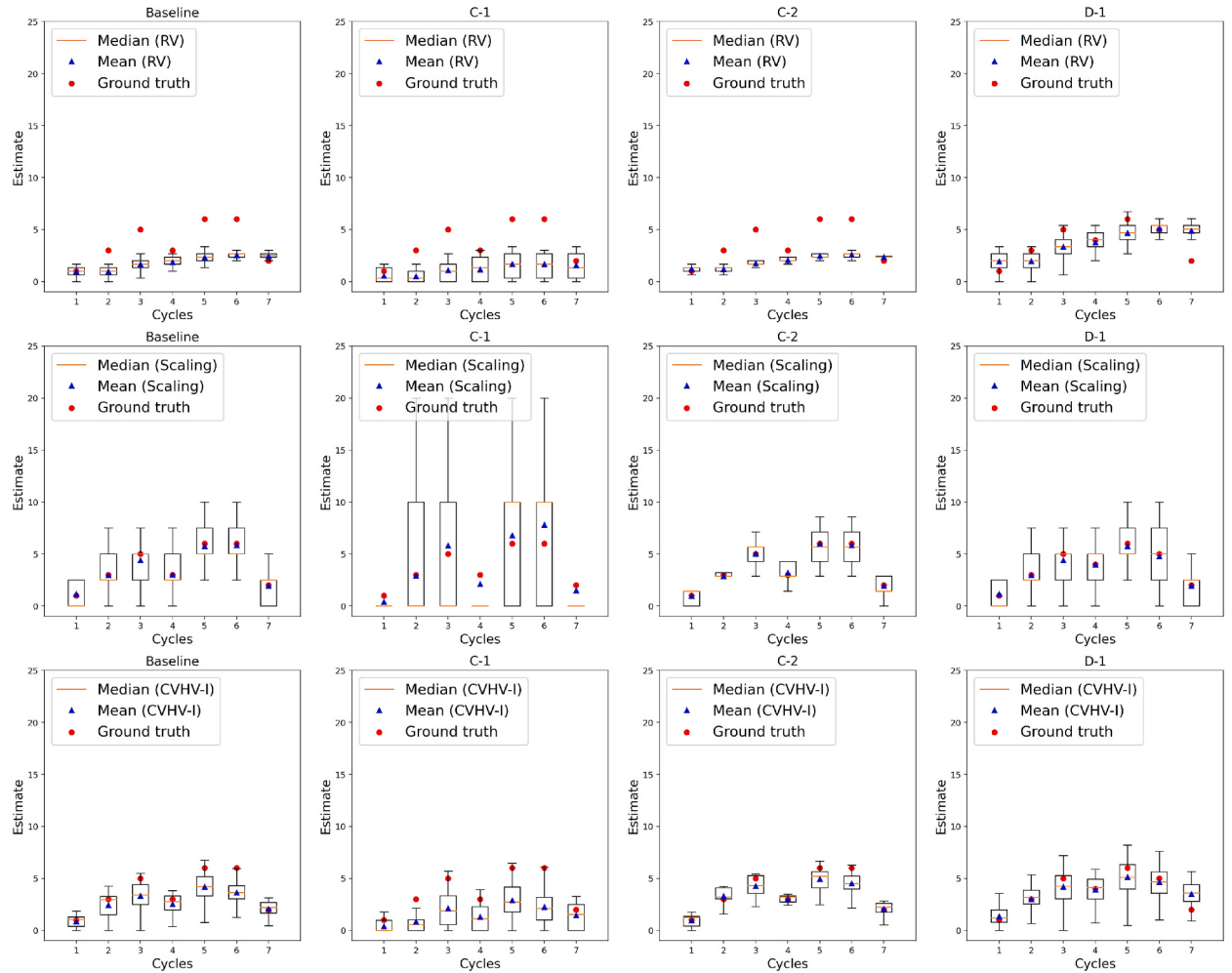


Fig. 6. Boxplots of the estimates of the numbers of holding vehicles based on the CVHV-I sub-model for the period 12:45–13:00.

total number of vehicles in a lane at an instant of interest can be established:

$$D = \eta + \bar{q}(1 - \bar{p}) \frac{l}{v_f} + R, \quad (76)$$

where D represents the total number of vehicles in the lane at the instant of interest; η is the number of new CVs in the lane at the instant of interest; the second term in Eq. (76) represents the expected number of new NCs in the lane at the instant of interest; and R is the number of holding vehicles in the lane at the instant of interest, which is estimated using the proposed CVHV model. The holding vehicle-based method described in Eq. (76), referred to as the HV method, was applied herein to estimate the total number of vehicles in a lane at an instant of interest.

The scaling method and the EVLS algorithm were employed as benchmark methods for comparison with the HV method. To unleash the full potential of the scaling method and the EVLS algorithm, the true CV penetration rates were used in both methods to estimate the total number of vehicles in a lane. All three methods were applied to the simulation cases described in Section 4, which encompass various combinations of signal timings, V/C ratios, CV penetration rates, and instants of interest. The ground truths of the total number of vehicles in a lane at the instants of interest were recorded for evaluation. Consistent with earlier analyses, RMSE, MAE, and VoD were used as evaluation metrics.

Tables 6 and 7 summarize the results of estimating the total number of vehicles in a lane at instants of interest falling within the effective red or effective green of a signal group, respectively. These results demonstrate that the proposed HV method significantly outperformed both the EVLS algorithm and the scaling method across all evaluation metrics, highlighting the critical role of accurately estimating the number of holding vehicles in advancing other useful traffic state estimation methods.

Figs. 10 and 11 illustrate the results presented in Tables 6 and 7, respectively. The proposed HV method produced more concentrated and well-distributed patterns, clearly confirming its superiority. In contrast, the EVLS algorithm consistently tended to overestimate the total number of vehicles, as expected, while the scaling method showed substantial estimation variability.

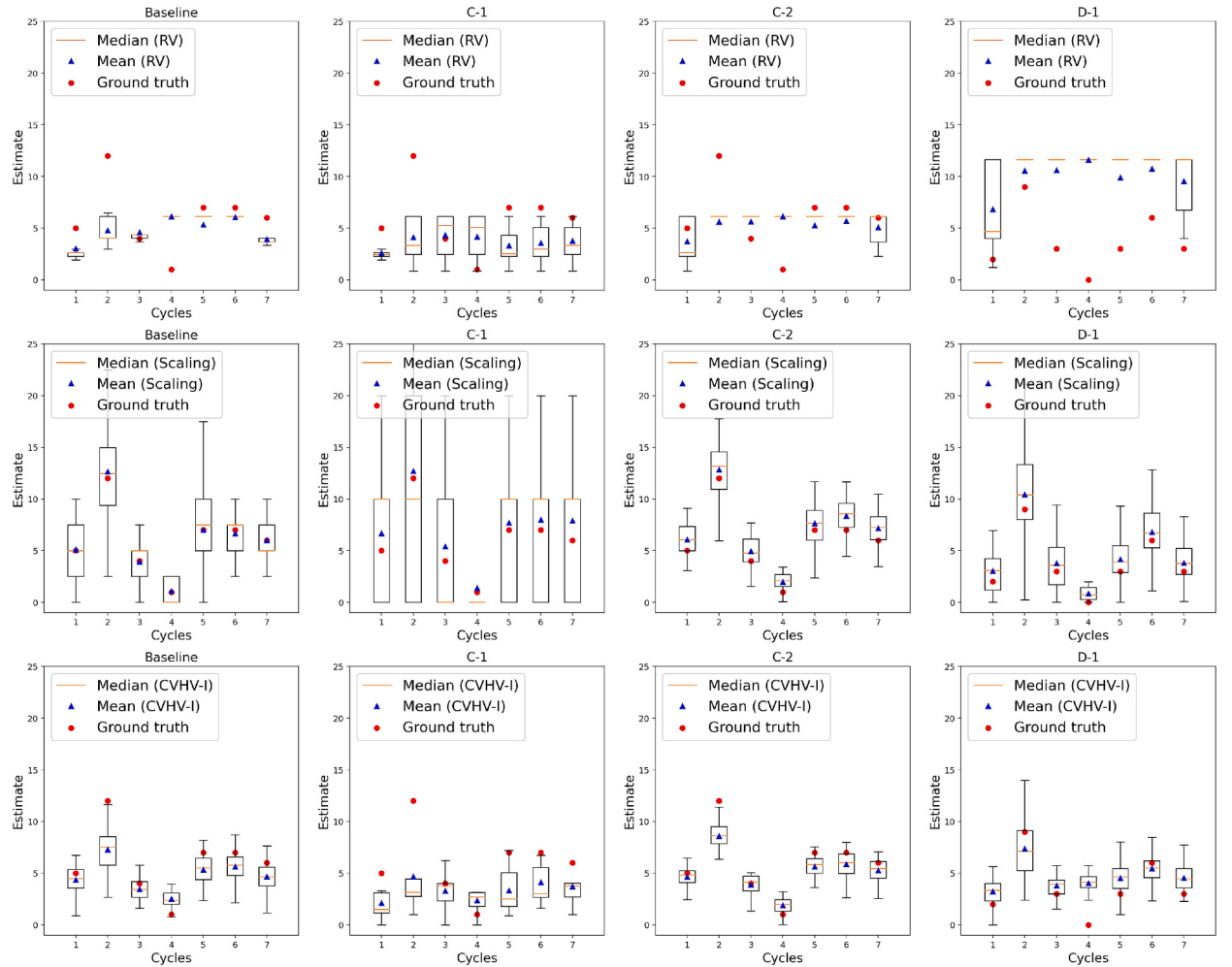


Fig. 7. Boxplots of the estimates of the numbers of holding vehicles based on the CVHV-I sub-model for the period 16:00–16:15.

Table 5

Performance of the CVHV-II sub-model in estimating numbers of holding vehicles based on NGSIM data.

Period	Case	α	θ	RMSE			MAE			VoD			
				RV	Scaling method	CVHV-II	RV	Scaling method	CVHV-II	RV	Scaling method	CVHV-II	
12:45	Baseline	0.4	0.5	—	1.39	1.30	—	1.01	0.92	—	1.77	1.64	
	—	C-1	0.1	0.5	—	3.62	1.63	—	2.08	1.14	—	13.06	2.29
	13:00	G-2	0.7	0.5	—	0.93	0.82	—	0.75	0.54	—	0.60	0.59
	—	D-1	0.4	1	0.61	0.47	0.29	0.58	0.17	0.09	0.17	0.22	0.08
16:00	Baseline	0.4	0.5	—	0.53	0.47	—	0.37	0.14	—	0.23	0.21	
	—	C-1	0.1	0.5	—	1.22	1.00	—	0.45	0.36	—	1.42	0.94
	16:15	G-2	0.7	0.5	—	0.38	0.29	—	0.31	0.09	—	0.09	0.09
	—	D-1	0.4	1	2.38	2.07	1.69	2.07	1.70	1.37	1.37	4.31	1.29

Collectively, these findings further highlight the importance of accurately estimating the number of holding vehicles.

6.2. A simple illustrative example of CV-based adaptive signal control

In traffic signal control, the number of holding vehicles at the end of a cycle directly provides the initial state for the next cycle, making it an essential input for estimating traffic delays. A simple illustrative example of CV-based adaptive signal control using the VISSIM platform is presented in this subsection to demonstrate the significance of accurately modeling holding vehicles.

Consider a crossroad with two approaching lanes. Each lane was controlled by a signal group. A standard red-green-amber signal structure was applied, with a fixed amber duration of 3 s. The cycle length was set to 60 s for simplicity, and the clearance times and

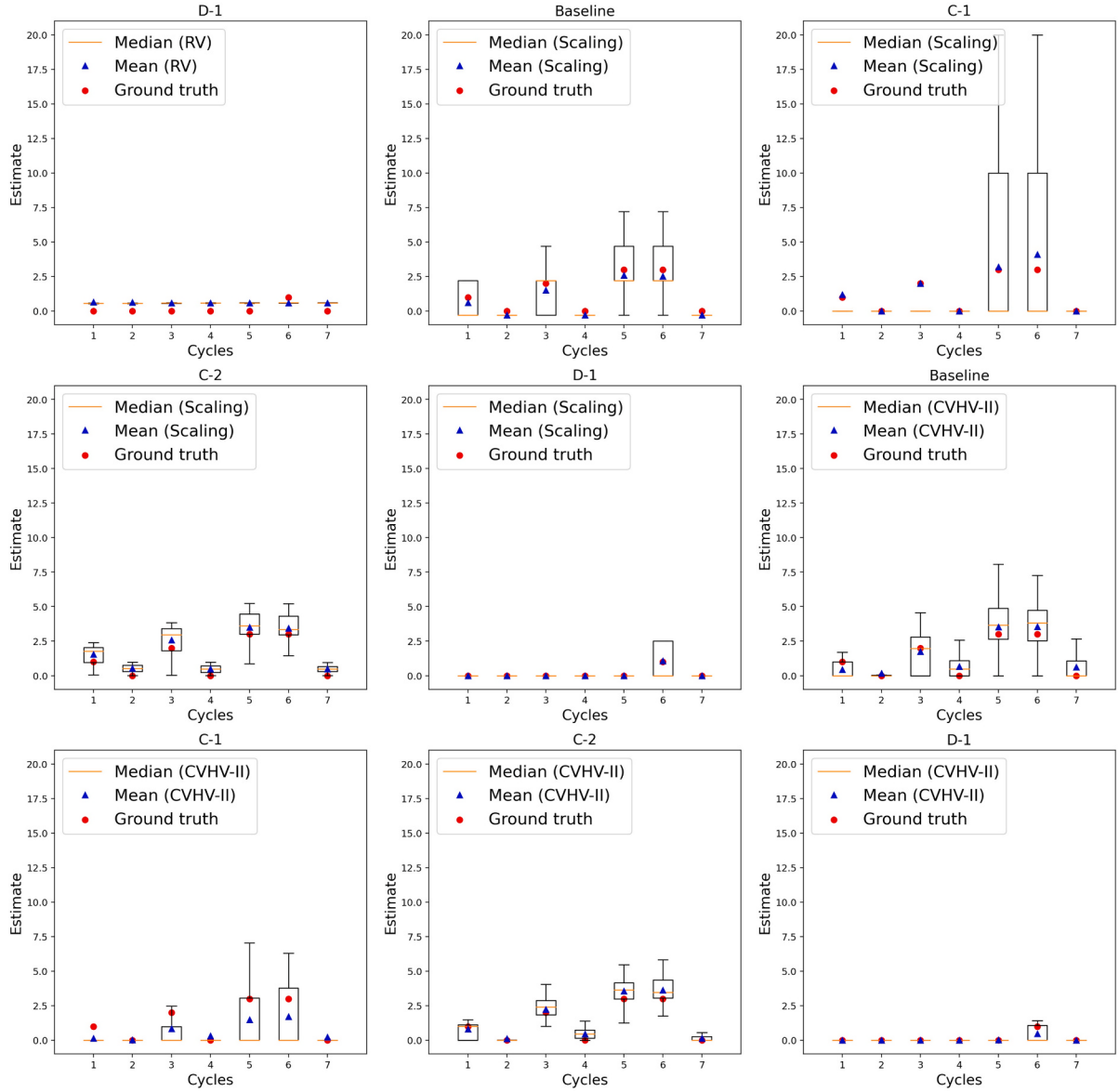


Fig. 8. Boxplots of the estimates of the numbers of holding vehicles based on the CVHV-II sub-model for the period 12:45–13:00.

minimum green durations were both fixed at 5 s. Without loss of generality, the start of a cycle was defined as the beginning of the effective red for signal group 1, resulting in the end of a cycle occurring during the effective green for signal group 1 and the effective red for signal group 2. Accordingly, the CVHV-I and CVHV-II models were applied to estimate the number of holding vehicles for lanes 1 and 2 at the end of each cycle. Symmetric (i.e., 500 veh/h and 500 veh/h) and asymmetric (i.e., 1200 veh/h and 600 veh/h) average demand scenarios were considered. Given that the saturation headway was determined to be 1.59 s, these scenarios represented varying congestion levels, with V/C ratios at the intersection of approximately 0.51 and 0.92 for the symmetric and asymmetric demand scenarios, respectively. To simulate stochastic traffic demand, the actual vehicle arrivals followed Poisson distributions. Each vehicle was randomly assigned to be either a CV, with a probability of π (the true CV penetration rate), or an NC, with a probability of

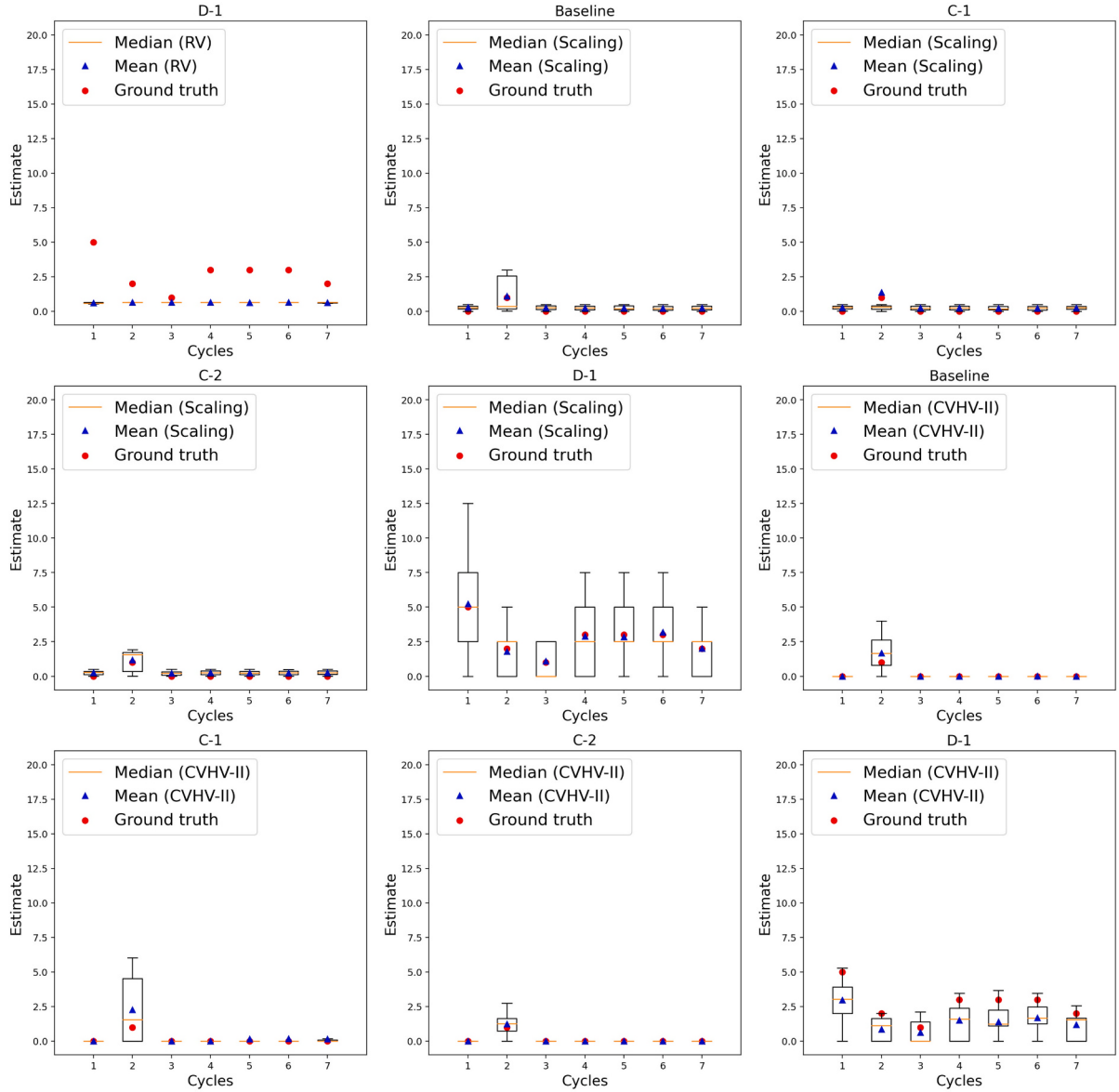


Fig. 9. Boxplots of the estimates of the numbers of holding vehicles based on the CVHV-II sub-model for the period 16:00–16:45.

Table 6

Performance of the HV method in estimating the total number of vehicles in a lane based on the CVHV-I sub-model.

Case	r	V/C	μ	φ	EVLS	RMSE Scaling method	HV	EVLS	MAE Scaling method	HV	EVLS	VoD Scaling method	HV
Baseline	30	0.5	0.4	0.5	6.39	4.59	3.17	4.72	3.68	2.49	38.50	21.04	10.05
A-1	15	0.5	0.4	0.5	6.21	5.21	4.88	4.76	4.18	3.76	38.44	27.16	22.86
A-2	45	0.5	0.4	0.5	5.39	3.34	2.23	3.48	2.61	1.75	28.03	11.11	4.69
B-1	30	0.3	0.4	0.5	4.68	3.48	2.84	3.32	2.76	2.24	21.69	12.14	7.96
B-2	30	0.7	0.4	0.5	6.67	5.19	3.52	5.12	4.08	2.77	43.05	27.02	12.11
B-3	30	0.95	0.4	0.5	7.40	6.27	3.73	5.67	5.00	2.88	54.03	39.33	13.11
C-1	30	0.5	0.1	0.5	10.78	11.25	6.99	8.58	8.85	5.59	115.60	126.53	34.54
C-2	30	0.5	0.7	0.5	6.25	2.41	2.01	4.15	1.94	1.59	31.92	5.82	4.03
D-1	30	0.5	0.4	1	7.83	4.95	3.69	5.69	3.90	2.85	55.75	24.54	13.01

Table 7

Performance of the HV method in estimating the total number of vehicles in a lane based on the CVHV-II sub-model.

Case	r	V/C	γ	θ	RMSE		MAE			VoD			
					EVLS	Scaling method	HV	EVLS	Scaling method	HV	EVLS	Scaling method	HV
Baseline	30	0.5	0.4	0.5	4.41	4.38	3.42	3.42	3.42	2.69	19.41	19.17	11.64
A-1	15	0.5	0.4	0.5	4.85	4.86	4.21	3.79	3.82	3.33	23.33	23.44	17.04
A-2	45	0.5	0.4	0.5	3.87	3.31	2.55	2.80	2.61	1.96	14.68	10.91	5.88
B-1	30	0.3	0.4	0.5	3.17	3.21	2.76	2.50	2.56	2.21	10.08	10.33	7.53
B-2	30	0.7	0.4	0.5	6.01	5.15	3.95	4.56	4.10	3.10	35.72	26.56	14.81
B-3	30	0.95	0.4	0.5	9.59	6.31	4.03	7.22	4.97	3.16	76.47	39.84	14.66
C-1	30	0.5	0.1	0.5	10.40	10.39	6.90	8.13	8.12	5.65	108.24	108.13	35.44
C-2	30	0.5	0.7	0.5	2.40	2.34	2.17	1.85	1.86	1.75	5.78	5.51	4.72
D-1	30	0.5	0.4	1	4.20	4.19	3.24	3.33	3.31	2.58	17.62	17.52	10.51

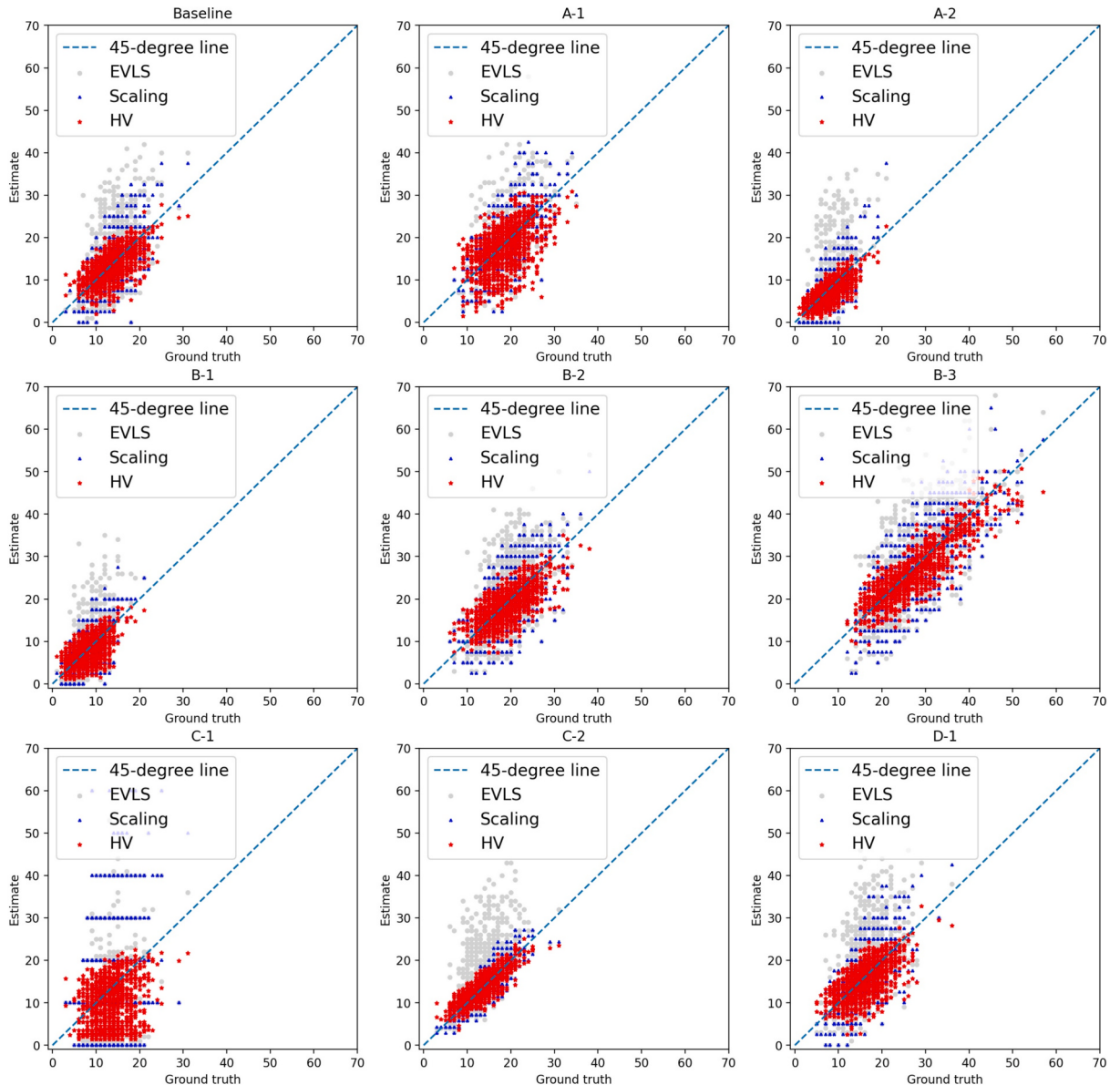


Fig. 10. Estimation accuracy of the HV method based on the CVHV-I sub-model.

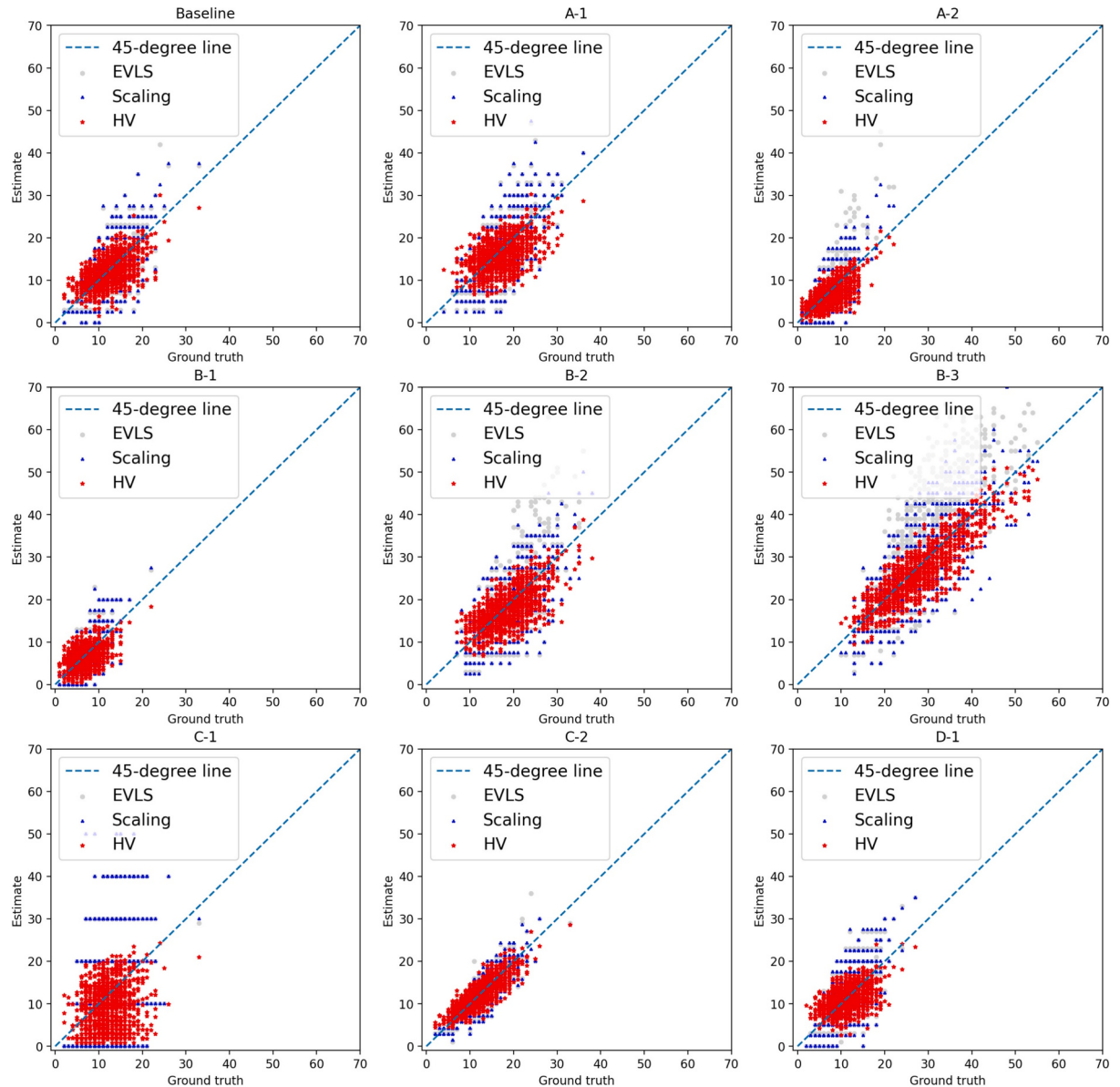


Fig. 11. Estimation accuracy of the HV method based on the CVHV-II sub-model.

$1 - \rho$, where ρ was given values of 0.1, 0.4, or 0.7. For each experiment, a 30-min warm-up period with fixed signal timings was simulated, followed by a 2-h study period where CV-based adaptive control schemes were simulated. The total intersection delay during the study period was recorded by VISSIM for further analysis.

At the end of cycle i , CV-based adaptive signal control optimizes signal timings for cycle $i+1$ by minimizing the total intersection delay in cycle $i+1$. Here, the total intersection delay was calculated as the sum of traffic delays across all lanes at the intersection. The real-time average vehicle arrival rate for lane $j, j \in \{1, 2\}$, during cycle $i+1$, denoted $\tilde{q}_{i+1,j}$, was estimated as

$$\tilde{q}_{i+1,j} = \frac{m_{i,j}}{C} + \bar{q}_{i,j} (1 - \bar{p}_{i,j}), \quad (77)$$

where $m_{i,j}$, C , $\bar{q}_{i,j}$, and $\bar{p}_{i,j}$ represent the number of CVs in lane j during cycle i ; the cycle length; the real-time average arrival rate in lane j during cycle i ; and the real-time average CV penetration rate in lane j during cycle i , respectively. Assuming a uniform vehicle arrival pattern with an arrival rate of $\tilde{q}_{i+1,j}$ and an initial state of $R_{i+1,j}, \forall j \in \{1, 2\}$, the traffic delay in lane $j, j \in \{1, 2\}$, during cycle $i+1$ was estimated as the area between the cumulative arrival and departure lines, $d_{i+1,j}$. The detailed derivations are provided in [Appendix B](#). Thus, the minimization objective was defined as $d_{i+1,1} + d_{i+1,2}$. It is evident that the numbers of holding vehicles at the end of a cycle, $R_{i+1,1}$ and $R_{i+1,2}$, serving as the initial states, are the critical inputs for estimating total intersection delay in CV-based adaptive signal control.

Three CV-based adaptive signal control schemes were evaluated: Schemes I, II, and III, which estimate the numbers of holding vehicles using the RV model, the scaling method, and the proposed CVHV model, respectively. All other settings were held the same across the three schemes. The adaptive signal optimization was formulated as

$$\begin{aligned} & \min_{g_{i+1,1}, g_{i+1,2}} d_{i+1,1} + d_{i+1,2} \\ & \text{s.t. } g_{i+1,1} + g_{i+1,2} = 52 \\ & g_{i+1,1} \geq 5 \\ & g_{i+1,2} \geq 5, \end{aligned} \quad (78)$$

where $g_{i+1,j}, j \in \{1, 2\}$, represents the actual green period in lane j during cycle $i+1$. A simple line search method with a step size of 1 s was applied to solve the optimization problem described in Eq. (78). Each scheme was implemented in VISSIM, with a 30-min warm-up period followed by a 2-h simulation during which signal timings were optimized at the end of each cycle. Total intersection delays during the study periods were recorded for evaluation.

[Table 8](#) summarizes the total intersection delays for different control schemes under varying traffic demands and CV penetration rates. These results show that the performance improved with increasing CV penetration rates for all schemes. Scheme I (RV model) exhibited superior performance compared with Scheme II (scaling method) in scenarios with low demand and low CV penetration rates. Conversely, Scheme II generally outperformed Scheme I in high-demand scenarios. Scheme III (CVHV model) consistently outperformed both Scheme I and Scheme II across all scenarios. [Fig. 12](#) visualizes the findings, emphasizing the superior performance of Scheme III and highlighting the critical importance of accurately estimating holding vehicles in CV-based adaptive signal control.

Table 8
Performance comparison of control schemes under varying traffic demands and CV penetration rates.

Traffic demand	ρ	Scheme I w/ RV	Total intersection delay (s) Scheme II w/ Scaling method	Scheme III w/ CVHV
500 veh/h and 500 veh/h	0.1	46,059	53,355	42,606
	0.4	44,474	44,803	40,858
1200 veh/h and 600 veh/h	0.7	42,171	41,070	38,645
	0.1	629,044	505,963	425,239
	0.4	508,887	466,746	417,146
	0.7	426,669	431,810	406,080

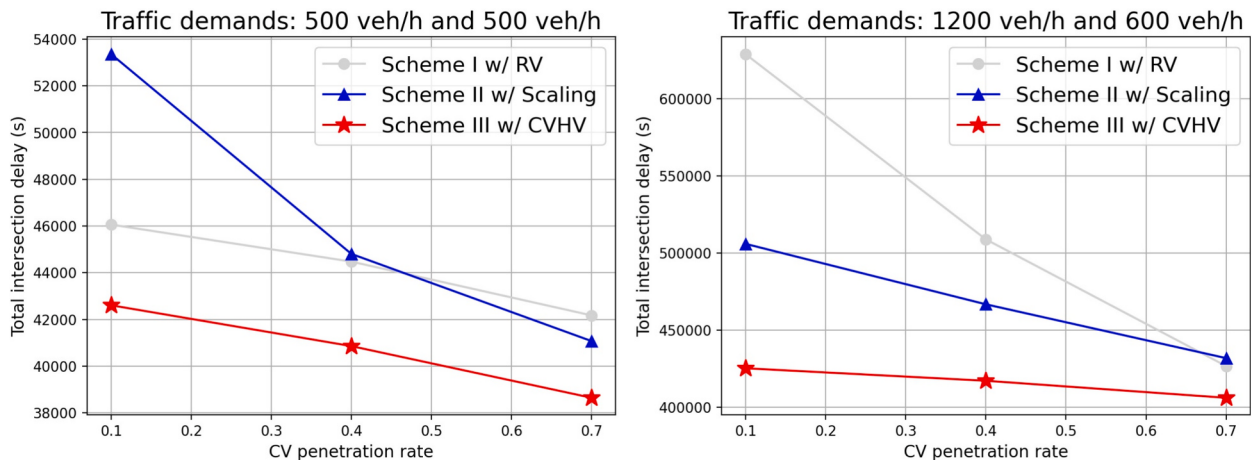


Fig. 12. Performance comparison across different CV-based adaptive signal control schemes.

7. Conclusion

Accurate estimation of the number of holding vehicles in all controlling lanes at any instant of interest is utmost importance for real-time traffic state monitoring and control. Advancements in CV technologies have revolutionized approaches for solving transportation problems and offered valuable opportunities for traffic monitoring using CV data. This paper developed a generic CVHV model that can estimate the numbers of holding vehicles under various signal timings, CV penetration rates, and V/C values. The models are entirely analytical and rely solely on CV data, making them highly practical for deployment. The model's effectiveness and applicability were validated through comprehensive VISSIM simulations and real-world experiments using the NGSIM dataset. These validations confirmed the robustness and accuracy of the CVHV model. Example applications of the CVHV model, including the estimation of the real-time total number of vehicles in a lane and an illustrative CV-based adaptive signal control, demonstrate the importance of accurately estimating the number of holding vehicles. Nevertheless, the proposed models do have some limitations: 1) the average effective vehicle length, a crucial parameter of the CVHV model, must be calibrated for accurate estimation in real-world applications; and 2) the model depends on average arrival rate and CV penetration rate as inputs, which means that the estimated number of holding vehicles is an expected value without accounting for its uncertainty.

Beyond adaptive signal control, the concept of holding vehicles offers potential for a wider range of traffic management applications. As a generalizable framework, it could be applied to scenarios where vehicles are impeded or delayed, such as dynamic lane management, ramp metering, or traffic incident detection. These applications could leverage the number of holding vehicles as a real-time indicator of congestion, enhancing traffic efficiency across diverse systems. Future work will focus on integrating the CVHV model into real-time traffic signal control systems and exploring its broader applicability, further enhancing traffic efficiency and management.

CRediT authorship contribution statement

Shaocheng Jia: Writing – original draft, Writing – review & editing, Conceptualization, Methodology, Software, Data curation, Formal analysis, Validation. **S.C. Wong:** Validation, Supervision, Project administration, Funding acquisition, Writing – review & editing, Methodology, Conceptualization, Resources. **Wai Wong:** Conceptualization, Validation, Writing – review & editing.

Declaration of Competing Interest

The authors declare that they have no known competing financial interests or personal relationships that could have appeared to influence the work reported in this paper.

Acknowledgments

The first author was supported by a Postgraduate Scholarship from The University of Hong Kong. The second author was supported by the Research Grants Council of the Hong Kong Special Administrative Region, China (Project Nos.: 17204919 and 17205822), and the Francis S Y Bong Professorship in Engineering.

Appendix

Appendix A. Algorithm 1

Algorithm 1 proposed in Jia et al. (2023) is presented as follows:

Algorithm 1: Computing $\{\tilde{P}(N = k, M = i)\}$ and $\{W(N = k, M = i)\}$, $\forall k \in \mathbb{N}^+, i \in [1, k]$.

```

1: Initialization:  $\{\tilde{P}(N = 1, M = 1)\} \leftarrow \{f(0; \bar{q}\tau)\}$ ,  $\{W(N = 1, M = 1)\} \leftarrow \{1\}$ .
2: For  $k$  in  $\mathbb{N}^+ \setminus \{1\}$  do
3:   For  $i$  in  $\{1, 2, 3, \dots, k\}$  do
4:     If  $i < k$  then
5:       For  $l$  in  $\{1, 2, 3, \dots, k-i\}$  do
6:         If  $l = 1$  then
7:            $\{\tilde{P}(N = k, M = i)\} \leftarrow f(l; \bar{q}i\tau) \bullet \{\tilde{P}(N = k-i, M = l)\}$ 
8:            $\{W(N = k, M = i)\} \leftarrow \{W(N = k-i, M = l)\}$ 
9:         Else
10:          For each value in  $f(l; \bar{q}i\tau) \bullet \{\tilde{P}(N = k-i, M = l)\}$  do
11:            If value  $\in \{\tilde{P}(N = k, M = i)\}$  then
12:              Find  $j$  such that  $\tilde{P}_j(N = k, M = i) = \textit{value}$ 
13:               $W_j(N = k, M = i) \leftarrow W_j(N = k, M = i) + 1$ 
14:            Else
15:               $\{\tilde{P}(N = k, M = i)\} \leftarrow \{\tilde{P}(N = k, M = i)\} + \{\textit{value}\}$ 
16:               $\{W(N = k, M = i)\} \leftarrow \{W(N = k, M = i)\} + \{1\}$ 
17:            End if
18:          End for
19:        End if
20:      End for
21:    Else
22:       $\{\tilde{P}(N = k, M = i)\} \leftarrow \{f(0; \bar{q}i\tau)\}$ 
23:       $\{W(N = k, M = i)\} \leftarrow \{1\}$ 
24:    End if
25:  End for
26: End for
27: Output:  $\{\tilde{P}(N = k, M = i)\}$  and  $\{W(N = k, M = i)\}$ ,  $\forall k \in \mathbb{N}^+, i \in [1, k]$ .

```

Appendix B. Real-time delay estimation for CV-based adaptive signal control

This appendix derives the real-time traffic delays for cycle $i+1$ in lanes 1 and 2, denoted as $d_{i+1,2}$ and $d_{i+1,1}$, under the assumption of uniform vehicle arrivals. As illustrated in Fig. B1, traffic delays can be estimated as the areas between the cumulative arrival and departure lines. Using geometric principles, $d_{i+1,2}$ and $d_{i+1,1}$ are derived as follows:

$$d_{i+1,1} = \begin{cases} R_{i+1,1}r_{i+1,1} + \frac{\tilde{q}_{i+1,1}r_{i+1,1}^2}{2} + \frac{\left(R_{i+1,1} + \tilde{q}_{i+1,1}r_{i+1,1}\right)^2}{2\left(s - \tilde{q}_{i+1,1}\right)}, & \text{if } \tilde{q}_{i+1,1} \leq \frac{sg_{i+1,1} - R_{i+1,1}}{C} \\ \left(2R_{i+1,1} + \tilde{q}_{i+1,1}r_{i+1,1}\right)r_{i+1,1} + g_{i+1,1} \left[2R_{i+1,1} + \tilde{q}_{i+1,1}(2C - g_{i+1,1}) - sg_{i+1,1}\right], & \text{if } \tilde{q}_{i+1,1} > \frac{sg_{i+1,1} - R_{i+1,1}}{C} \end{cases}, \quad (\text{B1})$$

$$d_{i+1,2} = \begin{cases} \frac{1}{2} \left(2R_{i+1,2} + \tilde{q}_{i+1,2}r_0 \right) r_0 + \frac{\left(R_{i+1,2} + \tilde{q}_{i+1,2}r_0 \right)^2}{2\left(s - \tilde{q}_{i+1,2} \right)} + \frac{1}{2}\tilde{q}_{i+1,2}(r_{i+1,2} - r_0)^2, & \text{if } \tilde{q}_{i+1,2} \leq \frac{sg_{i+1,2} - R_{i+1,2}}{r_0 + g_{i+1,2}}, \\ \frac{1}{2} \left(2R_{i+1,2} + \tilde{q}_{i+1,2}C \right) C - \frac{1}{2} \left(2C - g_{i+1,2} - 2r_0 \right) sg_{i+1,2}, & \text{if } \tilde{q}_{i+1,2} > \frac{sg_{i+1,2} - R_{i+1,2}}{r_0 + g_{i+1,2}} \end{cases}, \quad (\text{B2})$$

where $r_{i+1,j}$, $g_{i+1,j}$, $\tilde{q}_{i+1,j}$, s , C , r_0 , and $R_{i+1,j}$, respectively, represent the effective red in cycle $i+1$ in lane j ; the effective green in cycle $i+1$ in lane j ; the estimated real-time average arrival rate in cycle $i+1$ in lane j ; the saturation flow rate; the cycle length; the clearance loss time (4 s in this case); and the number of holding vehicles in cycle $i+1$ in lane j estimated by the RV model (Scheme I), the scaling method (Scheme II) or the CVHV model (Scheme III).

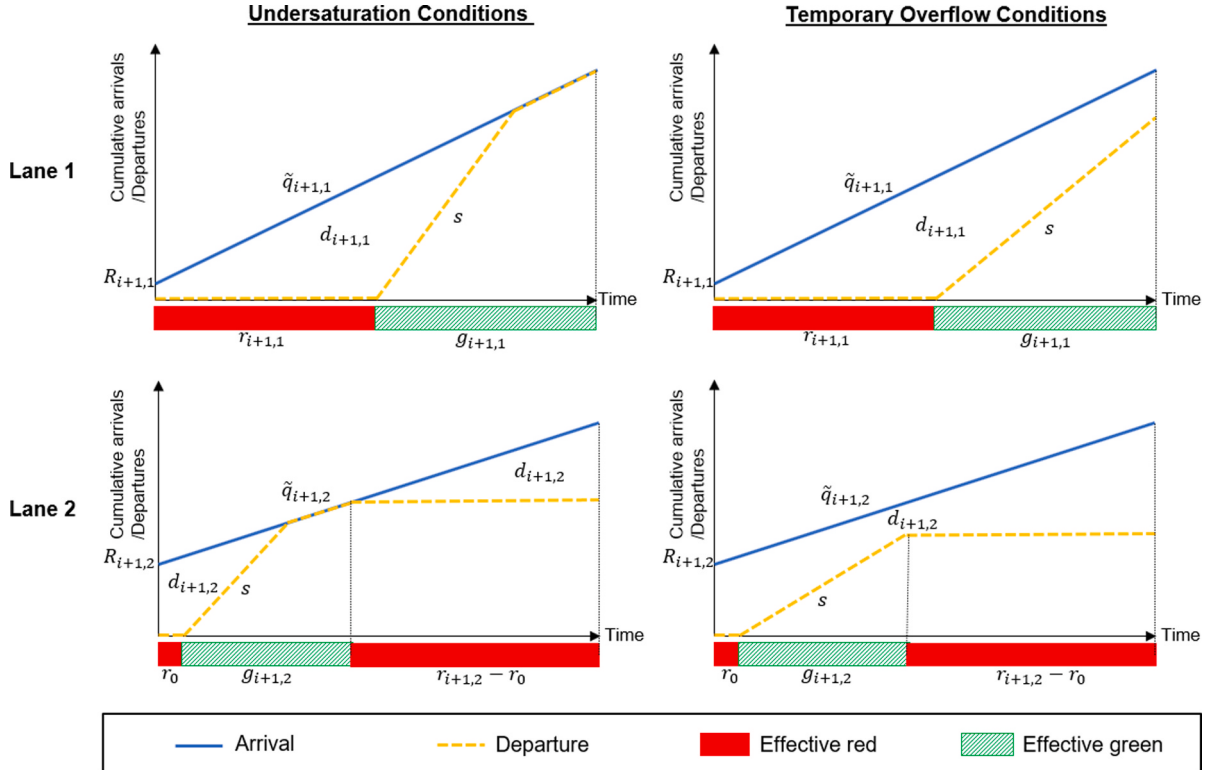


Fig. B1. Real-time delay estimation in CV-based adaptive signal control.

References

- Ambühl, L., Menendez, M., 2016. Data fusion algorithm for macroscopic fundamental diagram estimation. *Transp. Res. Part C Emerging Technol.* 71, 184–197.
- Cao, Y., Tang, K., Sun, J., Ji, Y., 2021. Day-to-day dynamic origin–destination flow estimation using connected vehicle trajectories and automatic vehicle identification data. *Transp. Res. Part C Emerging Technol.* 129, 103241.
- Comert, G., 2013. Simple analytical models for estimating the queue lengths from probe vehicles at traffic signals. *Transp. Res. B Methodol.* 55, 59–74.
- Comert, G., 2016. Queue length estimation from probe vehicles at isolated intersections: Estimators for primary parameters. *Eur. J. Oper. Res.* 252, 502–521.
- Comert, G., Cetin, M., 2009. Queue length estimation from probe vehicle location and the impacts of sample size. *Eur. J. Oper. Res.* 197, 196–202.
- Comert, G., Cetin, M., 2011. Analytical evaluation of the error in queue length estimation at traffic signals from probe vehicle data. *IEEE Trans. Intell. Transp. Syst.* 12, 563–573.
- Du, J., Rakha, H., Gayah, V.V., 2016. Deriving macroscopic fundamental diagrams from probe data: issues and proposed solutions. *Transp. Res. Part C Emerging Technol.* 66, 136–149.
- Federal Highway Administration, 2006. Next generation simulation: Peachtree Street dataset. Accessed June 25, 2022, <https://data.transportation.gov/Automobiles/Next-Generation-Simulation-NGSIM-Program-Peachtree/mupt-aksf>.
- Feng, Y., Head, K.L., Khoshmagham, S., Zamanipour, M., 2015. A real-time adaptive signal control in a connected vehicle environment. *Transp. Res. Part C Emerging Technol.* 55, 460–473.
- Geroliminis, N., Daganzo, C.F., 2008. Existence of urban-scale macroscopic fundamental diagrams: some experimental findings. *Transp. Res. B Methodol.* 42 (9), 759–770.

- Hao, P., Ban, X.J., Guo, D., Ji, Q., 2014. Cycle-by-cycle intersection queue length distribution estimation using sample travel times. *Transp. Res. B Methodol.* 68, 185–204.
- Iqbal, M.S., Hadi, M., Xiao, Y., 2018. Effect of link-level variations of connected vehicles (CV) proportions on the accuracy and reliability of travel time estimation. *IEEE Trans. Intell. Transp. Syst.* 20 (1), 87–96.
- Jenelius, E., Koutsopoulos, H.N., 2013. Travel time estimation for urban road networks using low frequency probe vehicle data. *Transp. Res. B Methodol.* 53, 64–81.
- Jenelius, E., Koutsopoulos, H.N., 2015. Probe vehicle data sampled by time or space: Consistent travel time allocation and estimation. *Transp. Res. B Methodol.* 71, 120–137.
- Jia, S., Wong, S.C., Wong, W., 2023. Uncertainty estimation of connected vehicle penetration rate. *Transp. Sci.* 57 (5), 1160–1176.
- Jia, S., Wong, S.C., Wong, W., 2024a. Modeling residual-vehicle effects on uncertainty estimation of the connected vehicle penetration rate. *Transp. Res. Part C Emerging Technol.* 168, 104825.
- Jia, S., Wong, S.C., Wong, W., 2024b. Modeling residual-vehicle effects in undersaturation conditions on uncertainty estimation of the connected vehicle penetration rate. In: *The 25th International Symposium on Transportation and Traffic Theory*, 15–17 July, Michigan, USA.
- Jia, S., Wong, S.C., Wong, W., 2025. Adaptive signal control at partially connected intersections: a stochastic optimization model for uncertain vehicle arrival rates. *Transp. Res. B Methodol.* 193, 103161.
- Khan, S.M., Dey, K.C., Chowdhury, M., 2017. Real-time traffic state estimation with connected vehicles. *IEEE Trans. Intell. Transp. Syst.* 18 (7), 1687–1699.
- Lu, Y., Xu, X., Ding, C., Lu, G., 2019. A speed control method at successive signalized intersections under connected vehicles environment. *IEEE Intell. Transp. Syst. Mag.* 11 (3), 117–128.
- Meng, F., Wong, S.C., Wong, W., Li, Y.C., 2017. Estimation of scaling factors for traffic counts based on stationary and mobile sources of data. *Int. J. Intell. Transp. Syst. Res.* 15 (3), 180–191.
- Mousa, S.R., Ishak, S., 2017. An extreme gradient boosting algorithm for freeway short-term travel time prediction using basic safety messages of connected vehicles. In: *Transportation Research Board 96th Annual Meeting*, 2017, Washington, DC, United States.
- Rahmani, M., Jenelius, E., Koutsopoulos, H.N., 2015. Non-parametric estimation of route travel time distributions from low-frequency floating car data. *Transp. Res. Part C Emerging Technol.* 58, 343–362.
- Tahir, M.N., Katz, M., 2022. Performance evaluation of IEEE 802.11 p, LTE and 5G in connected vehicles for cooperative awareness. *Eng. Rep.* 4 (4), e12467.
- Tian, D., Yuan, Y., Qi, H., Lu, Y., Wang, Y., Xia, H., He, A., 2015. A dynamic travel time estimation model based on connected vehicles. *Math. Probl. Eng.* 2015, 903962.
- Varaiya, P., 2013. Max pressure control of a network of signalized intersections. *Transp. Res. Part C Emerging Technol.* 36, 177–195.
- Wang, P., Zhang, J., Deng, H., Zhang, M., 2020. Real-time urban regional route planning model for connected vehicles based on V2X communication. *J. Transp. Land Use* 13 (1), 517–538.
- Wong, W., Wong, S.C., 2015. Systematic bias in transport model calibration arising from the variability of linear data projection. *Transp. Res. B Methodol.* 75, 1–18.
- Wong, W., Wong, S.C., 2016a. Biased standard error estimations in transport model calibration due to heteroscedasticity arising from the variability of linear data projection. *Transp. Res. B Methodol.* 88, 72–92.
- Wong, W., Wong, S.C., 2016b. Evaluation of the impact of traffic incidents using GPS data. *Proceedings of the Institution of Civil Engineers – Transport* 169(3), 148–162.
- Wong, W., Wong, S.C., 2016c. Network topological effects on the macroscopic Bureau of Public Roads function. *Transportmetrica a: Transport Science* 12 (3), 272–296.
- Wong, W., Wong, S.C., 2019. Unbiased estimation methods of nonlinear transport models based on linearly projected data. *Transp. Sci.* 53 (3), 665–682.
- Wong, W., Wong, S.C., Liu, X., 2019a. Bootstrap standard error estimations of nonlinear transport models based on linearly projected data. *Transportmetrica a: Transport Science* 15 (2), 602–630.
- Wong, W., Shen, S., Zhao, Y., Liu, X., 2019b. On the estimation of connected vehicle penetration rate based on single-source connected vehicle data. *Transp. Res. B Methodol.* 126, 169–191.
- Wong, W., Wong, S.C., Liu, X., 2021. Network topological effects on the macroscopic fundamental diagram. *Transportmetrica b: Transport Dynamics* 9 (1), 376–398.
- Yang, X., Lu, Y., Hao, W., 2017. Origin-destination estimation using probe vehicle trajectory and link counts. *J. Adv. Transp.* 2017, 4341532.
- Yin, Y., 2008. Robust optimal traffic signal timing. *Transp. Res. B Methodol.* 42 (10), 911–924.
- Zhao, Y., Zheng, J., Wong, W., Wang, X., Meng, Y., Liu, H.X., 2019a. Estimation of queue lengths, probe vehicle penetration rates, and traffic volumes at signalized intersections using probe vehicle trajectories. *Transp. Res. Rec.* 2673 (11), 660–670.
- Zhao, Y., Zheng, J., Wong, W., Wang, X., Meng, Y., Liu, H.X., 2019b. Various methods for queue length and traffic volume estimation using probe vehicle trajectories. *Transp. Res. Part C Emerging Technol.* 107, 70–91.
- Zhao, Y., Wong, W., Zheng, J., Liu, H.X., 2022. Maximum likelihood estimation of probe vehicle penetration rates and queue length distributions from probe vehicle data. *IEEE Trans. Intell. Transp. Syst.* 23 (7), 7628–7636.